J. Indian Inst. Sci., Sept.–Oct. 1990, **70**, 455–491.

IISc THESES ABSTRACTS

Thesis Abstract (Ph.D.)

Antibodies specific to deoxyribo-, mono-, di- and trinucleotides: Sequence-dependent binding to dsDNA by Neelam Suri.
Research supervisors: T. M. Jacob and N. Appaji Rao.
Department: Biochemistry.

1. Introduction

Nucleic acids and their components are not immunogenic by themselves. Antibodies which react with nucleic acids can be elicited against immunogens prepared by chemical coupling or electrostatic complexation of the nucleic-acid component with protein. Antibodies have been elicited against deoxyribomono-, di- and trinucleotides in our laboratory[1]. Hapten-binding populations of these antibodies were specific to the total structure of the hapten. Their binding to the respective radiolabelled hapten could not be competed with native DNA, whereas denatured DNA could inhibit the binding though inefficiently. These results could be expected as the bases are fairly buried inside a DNA double helix. It was later discovered in our laboratory that antibodies raised against dpG, dpC, dpA, dpApT and dpTpA had populations that could bind to dsDNA with nucleotide specificity[2,3]. After purification on dsDNA column, dpG antibodies showed much better binding to dsDNA compared to the same DNA in single-stranded form[4], thus showing that the double strandedness was not always a hindrance for the antibody binding, but had advantage sometimes over single-stranded structure arising from organisation of dsDNA. Further studies with dsDNA-binding populations of antibodies specific to deoxyribo- mono-, di- and trinucleotides were expected to be useful to throw more light on protein–DNA interactions.

2. Experimental programme

Antibodies were raised in two rabbits against the hapten, dpA, after coupling it chemically to proteins. One rabbit (R101) was first immunised with bovine serum albumin (BSA)-25dpA and reprimed with Limulus polyphemus hemocyanin (LPH)-730dpA. Second rabbit (R108) was immunised with LPH-730dpA from the beginning. dpApT, dpTpA and dTpTpAp antibodies were available in the laboratory from earlier work. To characterise the antibodies, ^{3}H-dpA, sheared *E. coli* ^{3}H-dsDNA and ^{3}H-ssDNA were used as probes in the nitrocellulose filter antibody binding assay (NFAB)[5]. The population of antibodies having high affinity to any of the radioactive probes could be studied in the presence of other populations. Specificities, affinities and antigenic determinants were determined by studying the binding to the respective labelled probes and estimating the efficiency of different unlabelled nucleosides, nucleotides, ds and ssDNA as inhibitors of binding. dsDNA-binding dpA antibodies were further studied using different dsDNAs including restriction fragments of phage and plasmid DNAs. Binding to restriction fragments of phage and plasmid DNAs was monitored by 'agarose gel electrophoresis'.

3. Main results and conclusions

IgG from R108 showed good binding to ^{3}H-dpA and ^{3}H-dsDNA and therefore was used for detailed investigations. Only dsDNA-binding property of R101 IgG was taken up for further studies as it had low ^{3}H-dpA-binding ability. Binding to ^{3}H-ssDNA was low in both the cases.

Populations of antibodies binding to both ^{3}H-dpA and ^{3}H-dsDNA from anti-dpA IgG-108 had high affinity to dpA and could discriminate it well from other deoxyribomononucleotides. The nucleoside part was immunodominant but the antibodies recognised the whole molecule of dpA and the linker region of the carrier protein. The antibodies had the stringent requirement for the presence of deoxyribose sugar for the binding. Both the populations of antibodies showed higher affinity to *E. coli* dsDNA compared to *E. coli* ssDNA.

Similar results were obtained for dsDNA-binding population from anti-dpA IgG-101, though it showed less stringency in discriminating between deoxyribose and ribose. Here the increase in dsDNA binding with increase in salt concentration indicated the involvement of hydrophobic interactions in binding.

One interesting observation made was that the binding of fixed input of sheared *E. coli* ^{3}H-dsDNA to increasing inputs of antibodies got saturated at lower inputs of anitibodies, when 85% of DNA was still unbound, and did not increase with increased input of antibodies. The unbound *E. coli* ^{3}H-dsDNA fragments recovered from the filtrate of NFAB assay were found to be deficient in binding to the antibodies. The results showed that most of the fragments of sheared *E. coli* dsDNA (50% A + T content) did not have the binding sites for dpA-specific antibodies. So the antibodies could be binding to very specific sequences containing dpA.

The number of binding sites for dpA antibodies in unit weights of eleven naturally occurring DNAs was found to be widely different by competition experiments. All these results pointed towards very specific binding sites for dpA antibodies. An attempt was made to indentify the binding sites by studying the direct binding to DNAs of known sequences by agarose gel electrophoresis assay. A computer analysis of the nucleotide sequences of all the unambiguously bound and unbound fragments revealed the presence of two unique hexanucleotide sequences, 1) $^{5'\text{TGATTT}\,3'}_{\text{ACTAAA}}$, 2) $^{5'\text{TTTCTG}\,3'}_{\text{AAAGAC}}$ in all the binding fragments and their absence in the non-binding fragments. More experiments are needed to firmly establish the involvement of these sequences and also to study which of the adenosine residue(s) in the sequences is involved in the binding.

Bases in dsDNA are sufficiently exposed in the major and minor grooves for base-specific interaction. Two hydrogen bonds with a base are sufficient to give base specificity for the interaction[6]. Looking at the immunodominant groups of dpA the possibilities are that 6-NH_2 group of adenine can form one hydrogen bond. N-1, C-2 and C-8 may be contributed by van der Waals interaction or substitution at these positions disturbs possible hydrophobic interactions. Interactions with deoxyribose and phosphate can give stability and nucleotide specificity. Interaction with deoxyribose could be by hydrogen bonding or van der Waals interaction. The phosphate group could interact through ionic interaction or hydrogen bonding. Fine structure of dsDNA at the binding site is expected to be an important factor in antibody binding, as complex formations based on weak interactions occur preferentially when the geometry of interacting molecules allow concerted formation of several weak bonds simultaneously.

Studies with dpApT, dpTpA and dTpTpAp antibodies also lead to the conclusion that they bind to double-stranded DNA at very specific sequences in which the respective hapten structure forms a part.

References

1. JACOB, T. M. AND SRIKUMAR, C	*J. Biosci.*, 1985, **7**, 61–73
2. JACOB, A. AND JACOB, T. M.	*Nucl. Acids Res.*, 1982, **10**, 6273–6280.
3. JACOB, A.	In *Double stranded DNA binding nucleotide antibodies - Studies on specificities, purification and binding to human chromosomes*, Ph.D. Thesis, Indian Institute of Science, Bangalore, India, 1984.
4. JACOB, A. AND JACOB, T. M.	*FEBS Lett.*, 1985, **189**, 81–84.
5. HUMAYUN, M. Z. AND JACOB, T. M.	*Biochim. Biophys. Acta*, 1973, **331**, 41–53.
6. SEEMAN, N. C., ROSENBERG, J. M. AND RICH, M.	*Proc. Natn. Acad. Sci USA*, 1976, **73**, 804–808.

Thesis Abstract (Ph.D.)

Vanadate-induced changes in hepatic calcium and calcium-dependent activities in the rat by Sharada Gullapalli.
Research supervisors: C. K. R. Kurup and T. Ramasarma.
Department: Biochemistry.

1. Introduction

The biochemical actions of vanadium, which has been recognized as an essential micronutrient element in plant and animal nutrition, are yet to be understood[1]. Vanadium salts inhibit Na^+, K^+–ATPase, stimulate plasma membrane-associated NADH oxidase and exhibit hormone-mimetic activity in cell cultures[2,3]. The effects of vanadate administration on the liver are poorly documented. The effects of vanadate on hepatic mitochondrial function in relation to calcium homeostasis are discussed in this work.

2. Materials and methods

Polyvanadate (4μmole/animal) was injected (i.p.) into rats and the animals were killed 1 h later. Adrenergic-receptor antagonists were administered 20 min prior to vanadate. Liver was perfused with 0.25 M sucrose for 5 or 10 min. Vanadate (100 μM) was added to the perfusing medium as indicated. Liver mitochondria were prepared by differential centrifugation. Oxidative phosphorylation and calcium-stimulated respiration under 'limited loading' conditions were determined by polarography. The activity of mitochondrial α-glycerophosphate dehydrogenase was determined using phenazine methosulphate and 2,6-dichlorophenol indophenol as electron acceptors[4].

3. Results and conclusions

A single intraperitoneal injection of polyvanadate to the rat resulted in a time- and dose-dependent increase of calcium-stimulated respiration by hepatic mitochondria. The optimum time was 1 h and dose 4μmol/rat (wt 120–130 g). This signified enhanced energy-dependent uptake of calcium by mitochondria, which was confirmed by measurement of [^{45}Ca] uptake. The possibility that enhanced uptake resulted from vanadate-influenced efflux of calcium from mitochondria *in vivo* was tested by

determination of the subcellular distribution of the metal ion. The data in Table I show that the concentration of calcium in the mitochondrial fraction decreased significantly on vanadate administration. The decrease was almost quantitatively accounted for by the increase in the cytosolic fraction The results indicated the occurrence of vanadate-mediated mobilization of mitochondrial calcium into the cytosol

Table I
Effect of administration of vanadate on the subcellular distribution of Ca^{2+} ions in rat liver

Subcellular fraction	ng ion calcium/g liver	
	Control	Vanadate treated
Nuclear	138 ± 20	111 ± 20
Mitochondrial	262 ± 42	171 ± 31*
Microsomal	237 ± 53	260 ± 35
Cytosolic	35 ± 5	93 ± 33*

Animals were injected (i.p.) with polyvanadate (4μmol/rat) and killed 1 h later Subcellular fractions were separated by differential centrifugation Perchloric-acid-soluble calcium was determined by atomic-absorption spectroscopy The values are the mean ± S. D. of six animals in each group.

*Significant ($P < 0.02$) control *vs* vanadate treated.

The stimulation of calcium-dependent respiration could be prevented by prior administration of α- but not of β-adrenergic antagonists. Sympathectomy did not affect the vanadate effect. These results suggested a possible direct interaction of vanadate with the α-adrenergic receptors on

Table II
Effect of polyvanadate administration to the rat on mitochondrial function

Activity	Treatment	Control	Vanadate treated
Calcium-stimulated respiration (ng atom O/mg protein)	*In vivo*	7.3 ± 1.0	13.1 ± 1.5*
	Perfusion	8.0 ± 0.1	11.9 ± 1.4*
Pyruvate dehydrogenase (n moles $K_3[Fe(CN)_6]$ reduced per min/mg protein)	*In vivo*	10.8 ± 1.5	5.3 ± 0.9*
	Perfusion	6.3 ± 0.4	3.2 ± 1.0*
α-Glycerophosphate dehydrogenase (n moles indophenol reduced/min/mg protein)	*In vivo*	11.6 ± 2.1	17.7 ± 2.4*
	Perfusion	13.5 ± 1.2	21.3 ± 2.3*

Animals were injected with polyvanadate (4μmol/rat; 1 h; '*in vivo*') or the livers were perfused with 0.25 M sucrose containing 100μM vanadate ('perfusion') for 10 min. Mitochondria were isolated and the activities assayed. Values are the mean ± SD of six animals in each group.

*Significance ($P < 0.01$) control *vs* vanadate treated.

hepatocyte plasma membrane. This was sought to be confirmed by perfusion of the liver with vanadate. The data presented in Table II show that perfusion of liver with vanadate reproduced the effects observed *in vivo*. The effects were not shown when the perfusing solution contained phenoxy benzamine (70 μg/ml), an α-adrenergic-receptor antagonist. Addition of the β-receptor antagonist propranolol (70 μg/ml) had no effect on vanadate-mediated changes. The decrease in pyruvate dehydrogenase activity on vanadate administration is consistent with the lowered calcium content of mitochondria as the enzyme is known to be calcium-regulated[5].

The increase in mitochondrial α-glycerophosphate dehydrogenase activity indicated the possibility that vanadate administration perturbed the thyroxine status of the animals. Measurements indicated that the hormone concentration increased in the liver.

Perfusion with vanadate caused a six-fold stimulation of the protein kinase C activity of hepatic plasma membrane. The cytosolic activity showed a 90% decrease. Perfusion with the α-adrenergic agonist phenylephrine showed similar changes in the activities of the membrane-associated and cytosolic enzymes.

This is the first demonstration of an α-adrenergic agonist mimicking action of vanadate *in vivo*.

References

1. UNDERWOOD, E. J. — *Trace elements in human health and disease*, Vol. 2, 1976, p. 269, Academic Press.
2. RAMASARMA, T. AND CRANE, F. L. — Does vanadium play a role in cellular regulation? *Curr. Topics Cellular Regulation*, 1981, **20**, 247–301.
3. JANDHYALA, B. S. AND HOM, G. J. — Physiological and pharmacological properties of vanadium, *Life Sci.*, 1983, **33**, 1325–1340
4. GULLAPALLI, S. — Vanadate-induced changes in calcium homeostasis in rat liver mitochondria, *ICSU Short Rep.*, 1986, **6**, 9321–9327.
5. DENTON, R. M. AND MCCORMACK, J. G. — Ca^{2+} as a second messenger within mitochondria, *TIBS*, 1986, **11**, 258–262.

Thesis Abstract (Ph.D.)

Development and application of immunoassays for monkey chorionic gonadotropin by Rabindranath Chakrabarti.
Research supervisor: A. Jagannadha Rao.
Department: Biochemistry.

1. Introduction

One of the most challenging problems in human pregnancy research is related to the events surrounding the blastocyst implantation, and initiation and regulation of chorionic gonadotropin (CG) secretion. During the last few decades, the macaques such as rhesus, cynomolgus and bonnet monkeys have been extensively used for studies of various problems in human reproduction[1-4].

A suitable method for early pregnancy diagnosis and quantitation of monkey CG(mCG) is of

paramount importance for studying the physiology of CG during early pregnancy, using macaques as model system. Non-availability of a purified preparation of mCG has precluded the development of a suitable homologous immunoassay for mCG. The existing liquid-phase radioimmunoassay (RIA)[5-7], hemagglutination inhibition test[8-11] and radioreceptor assay[12] suffer from one or more disadvantages such as less sensitivity, long assay time (24–30 hours), unreliability and high cost. Besides, CG is present in low levels and for short period (about 2 weeks) in the circulation in macaques.

Considering all the above facts, the present study was undertaken to develop a relatively less time-consuming, less expensive, simpler and highly sensitive immunoassays for mCG, using the bonnet monkey as experimental animal.

2. Experimental

2.1 *Animal and blood sampling*

Monkeys were maintained and blood samples were collected as previously described[7,13,14]. Adult cycling bonnet monkeys, having a mean (mean $\pm$ SE) cycle length 28 ± 2 days, were housed with selected proven fertile males from 9th day until the 14th day of menstrual cycle, and 12th day of cycle has been considered as day 1 of pregnancy. Blood samples were collected between 0900 and 1000 hours from saphenous vein, serum was separated and stored at -20°C until further processing.

2.2 *Assay for estradiol-17β* and progesterone

Serum samples were extracted and estradiol-17β and progesterone in the extracted samples were measured by specific RIA according to a procedure described earlier[7].

2.3 *Liquid-phase radioimmunoassay (RIA)* for CG

Antisera(a/s) to hCGβ- and oLHβ-subunits were raised and characterized for their titre, and cross-reactivity and specificity for mCG[7], using ^{125}I-hCG as the tracer. Using the most suitable oLHβ a/s(R24) and ^{125}I-hCG as the tracer, a liquid-phase RIA(LPRIA) for CG was standardized and used to determine the serum pattern of CG during early pregnancy in bonnet monkeys.

2.4 *Solid-phase RIA for CG*

Solid-phase RIA (SPRIA) for CG was developed by using epoxy-activated cellulose as the solid matrix. IgG from the oLHβ a/s(R24) was isolated by DEAE-cellulose chromatography[15], and covalently coupled to the epoxy-activated cellulose[16]. The SPRIA system consisted of IgG-coupled cellulose(2·5 μl/100 μl), 100 μl gelatin phosphate buffered saline, 100 μl ^{125}I-hCG(20,000–25,000 cpm) and hCG standards or serum samples(100–200 μl).

2.5 *Avidin-biotin micro-enzymeimmunoassay(AB-microEIA) for mCG*

The AB-microEIA for mCG was developed by using affinity-purified oLHβ IgG immobilized on microtitre well surface, biotinylated hCG as the tracer, pooled pregnant monkey serum(characterized for bioactive CG by mouse uterine weight assay) as the reference preparation for mCG, HRP-avidin as the enzyme marker and *O*-phenylene diamine as chromogen. But for enzyme-substrate reaction, all the reaction steps were carried out at 37°C in a humidified incubator.

2.6 *Experiments with GnRH analogues*

To test biopotencies of GnRH analogues, analogues were injected intravenously in adult male bonnet monkeys between 1000 and 1100 hours, and blood samples were collected at stipulated intervals and analyzed for testosterone by specific RIA.

A similar protocol was followed to examine the acute effects of Buserelin(100 μg/monkey) in pregnant bonnet monkeys on 31st day of fertile menstrual cycle. For examining the chronic effects, the same animals were administered Buserelin (2.4 μg/h) *via* alzet osmotic pumps implanted subcutaneously. The blood samples were collected daily for 9–11 days. All the serum samples were analysed for estradiol-17β and progesterone by RIA, and for mCG by the AB-microEIA.

3. Results and discussion

Of the several batches of hCGβ and oLHβ a/s tested, one batch of oLHβ a/s(R24) was found to be the most suitable and relatively specific for mCG. This a/s was chosen for all subsequent studies. The serum pattern of CG during early pregnancy in bonnet monkeys, determined by the LPRIA developed using this oLHβ a/s, was very much similar to those observed in rhesus monkeys[6]. However, the assay was less sensitive (detect CG between 28th and 30th day of fertile cycle) and time-consuming (24–30 h).

The assay time in the LPRIA (24–30 h) has been reduced considerably through the development of the SPRIA which needs only 6 hours for completion. Other advantages of the SPRIA, over the LPRIA, are that it is simple and easily standardizable, does not require any species-specific anti-immunoglobulin, and the cellulose-coupled IgG can be stored up to six months at 4°C without any loss of activity. The assay has been applied successfully to diagnose pregnancy in bonnet monkeys, with 86–100% accuracy between 28th and 30th day of fertile cycle. The serum non-specific inhibition in the SPRIA, found to be due to serum γ-globulin, was eliminated by keeping the serum concentration constant in all the assay tubes.

In spite of several advantages, the sensitivity of the SPRIA remained the same as that of the LPRIA. Thus, to improve sensitivity an AB-microEIA for CG, which combines the requirements of rapidity, simplicity and sensitivity and with a novel assay design was developed. Despite using the same oLHβ a/s in all three assays, the AB-microEIA was ten times more sensitive than SPRIA or LPRIA, implying that the assay design itself is responsible for increased sensitivity in the AB-microEIA. The assay time was only 5 hours. Another improvement in the assay design was the use of biologically active mCG reference preparation. The increased sensitivity of the AB-microEIA has permitted the diagnosis of pregnancy in bonnet monkeys four days earlier than by the LPRIA or SPRIA. The false CG positive results, obtained initially, were found to be due to serum γ-globulin, and were completely eliminated by prior heating of serum samples at 60°C for 30 min before use. The accuracy of the diagnosis was 98–100%.

The serum patterns of CG during early pregnancy in bonnet, cynomolgus and rhesus monkeys, determined by the AB-microEIA, were very similar to each other.

The application of the AB-microEIA was extended to monitor the changes in serum levels of CG following Buserelin injection in pregnant bonnet monkeys. Before injecting in pregnant monkeys, GnRH agonists were tested for their biopotency in monkeys using adult male bonnet monkeys as model system. It was found that there was a significant increase in serum levels within an hour following injection of GnRH agonists. The LH mediation of this effect was evident from the lack of

GnRH-stimulated testosterone increase in the presence of LH a/s. Of the several agonists tested, Buserelin was found to be the most potent one. It has been found that neither single injection nor continuous infusion of Buserelin had any effect on serum levels of CG in pregnant bonnet monkeys. It is possible that in these monkeys the luteo-placental shift has already been completed by the 31st day of fertile cycle resulting in dispensation of function of CG and hence dispensation of any regulatory mechanism for CG, and this perhaps could be the reason for not observing any effect of Buserelin on CG levels.

4. Conclusion

The present study clearly indicates that of the three immunoassays described here, the AB-microEIA is superior as far as rapidity, sensitivity, simplicity and cost are concerned, and it can effectively be used to study the events surrounding the blastocyst implantation, and initiation and regulation of chorionic gonadotropin secretion during early pregnancy in macaques. The present study also documents that the AB-microEIA can be used to detect and quantitate CG in a wide variety of non-human primates.

References

1. PRASAD, M. R. N. AND ANAND KUMAR, T. C. (eds) — *Use of non-human primates in biomedical research*, Indian National Science Academy, New Delhi, 1977.
2. ROONWAL, M. L., MOHANT, S. M. AND RATHORE, N. S. (eds) — *Current primate researches*, Department of Zoology, Jodhpur University, Jodhpur, India, 1984.
3. DICZFALUSY, E. AND STANDLY, C. C. (eds) — *The use of non-human primates in research on reproduction*, WHO Research and Training Centre on Human Reproduction, Karolinska Institute, Stockholm, 1972.
4. ANAND KUMAR, T. C. (ed.) — *Non-human primate models for study of human reproduction*, S. Karger, Basel, 1980.
5. ATKINSON, L. E., HOTCHKISS, J., FRITZ, G. R., SURVE, A. S. AND KNOBIL, E. — *Biol. Reprod.*, 1971, **5**, 95(Abs. 36).
6. HODGEN, D. G., TULLNER, W. W., VAITUKAITIS, J. L., WARD, D. N. AND ROSS, G. T — *J. Clin. Endocrinol. Metabolism.*, 1974, **39**, 457.
7. JAGANNADHA RAO, A. KOTAGI, S. G. AND MOUDGAL, N. R. — *J. Reprod. Fert.* 1984, **70**, 449–455.
8. HODGEN, G. D. AND ROSS, G. T. — *J. Clin. Endocrinol. Metabolism*, 1974, **38**, 927.
9. LEQUIN, R. M., ELVERS, L. H. AND BERTENS, A. P. M. G. — *J. Med. Primatol.*, 1981, **10**, 189–198.
10. STOUFFER, R. L. BONNETT, L. A., NIXON, W. E. AND HODGEN, G. D. — *Steroids*, 1977, **29**, 73–82.
11. NAQVI, R. H. AND LINDBERG, M. C. — *J. Med. Primatol.*, 1985, **14**, 229–233.
12. BOOHER, C. B., PRAHALADA, S. AND HENDRICKS, A. G. — *Am. J. Primatol.*, 1983, **4**, 45.

13.	MUKKU, V. R. AND MOUDGAL, N. R	In *Recent advances in reproduction and regulation of fertility* (Talwar G.P., ed.) 1979, p. 135, Elsevier/North-Holland.
14	PRAHALADA, S., MUKKU, V. P., JAGANNADHA RAO, A. AND MOUDGAL N. R.	*Contraception*, 1975, **12**, 137–147.
15.	FAHEY, J. L AND HORBETT, A. P.	*J. Biol. Chem.*, 1959, **234**, 2645–2651.
16	MURTHY, S. G. AND MOUDGAL, N. R	*52nd Annual Meeting of Society of Biological Chemists* (Abs. 555), India, 1983.

Thesis Abstract (Ph.D.)

The nucleocapsid protein, N and the haemagglutinin protein, H of the rinderpest virus: Production, characterization of monoclonal antibodies and application to the study of long-term persistence of the virus *in vitro* by K. Bhavani.
Research supervisor: M. S. Shaila.
Department: Microbiology and Cell Biology.

1. Introduction

Rinderpest is a natural infection of wild and domestic bovines in many parts of Africa and Asia. The causative agent, rinderpest virus, belongs to the Morbillivirus group of the family Paramyxoviridae; other members of the group include measles virus (MV), canine distemper virus (CDV) and peste-des-petits ruminant (PPR) virus. These viruses are known to cause chronic neurological diseases in their natural hosts. The basic mechanisms of human or animal diseases involving persistent viral infections are poorly understood at the cellular and molecular level. However, persistent infections can be established in a variety of cell lines and such cells can be used as a model system to study persistence[1].

Morbilliviruses are antigenically closely related and are monotypic[2]. The antigenic stability of these viruses is reflected on the epidemiology of the diseases they cause[3]. A life-long immunity against subsequent infections is induced after a generalised infection. Access to monoclonal antibodies has made it possible to identify a high frequence of occurrence of spontaneous and induced antigenic variations in these viruses. Possible epitopic changes occurring in the virus proteins during persistence *in vitro* can be studied in detail using monoclonal antibodies[4].

2. Experimental programme

The work is divided into three parts. The first deals with the production and characterization of RPV-specific H- and N-monoclonal antibodies. This involves fusion of mouse myeloma cells (SP_2/O) with sensitized B-lymphocytes from the spleen of BALB/c mouse immunized with RPV[5]. The antibody secreting clones were screened by enzyme-linked immunosorbant assay/radio immuno-assay (ELISA/RIA) and the antibodies were further characterized by RIPA and IF. Using competitive binding assay for all H- and N-specific antibodies, epitope analysis was done. Occurrence of these epitopes was detected in heterologous strains, *i.e.*, CDV and MV and sheep RPV.

The second part of the work describes the purification of H and F proteins from infected cell extracts using specific immuno-affinity columns. For H proteins, a monoclonal antibody was used

and for F protein, an F_1 antipeptide, aminoterminus antibody was used. The amino-acid composition was determined.

The third part of the work describes the fate of viral proteins H and F in Pi-2 cells when compared with acutely infected cells. The rate of synthesis of viral proteins N, H, F and M was studied using immunoprecipitation with antibodies and antigenic mapping of H and N proteins was carried out employing competitive binding assay. These epitopes could be delineated on the H proteins. Sites I and II overlap with each other and site III is distant from sites I and II. Two of the H-specific monoclonal antibodies showed virus neutralization property and all the nine H-monoclonal antibodies showed haemagglutination inhibition, although to different extent. Two epitopes could be identified on the N protein, and they are found to overlap with each other. When tested agaist MV, CDV and sheep RPV, the immunoreactivity of a given hybridoma was always more pronounced with respect to epitopes on the H proteins than on the N proteins. The site II-specific antibodies failed to react with sheep RPV and it also seems to vary in MV and CDV as seen by reduced ELISA titers.

Glycoproteins H and F were purified using specific immuno-affinity columns. They were copurified on a lentil-lectin sepharose-affinity column, but could not be further separated. To purify the H protein, a monoclonal antibody-affinity column was employed. Infected cytoplasmic extract was used as the protein source. By a single cycle of adsorption and desorption a highly purified H protein was obtained. SDS-PAGE of the eluted material, however, showed the presence of two proteins with M_r of 66,000 and 74,000. The M_r 66,000 protein was identified as the unglycosylated form of H protein, when infected cells were treated with tunicamycin (an inhibitor of glycosylation) and H protein immunoprecipitated using anti-H antibody. The amino-acid composition of H protein was determined. F protein was purified from the infected cell extract using an F_1-amino terminus-specific antipeptide-antibody-affinity column.

A detailed analysis of the virions, rinderpest viral protein, and establishment of persistent infection of RPV in Vero cells in culture (Pi-2) was earlier made in this laboratory. In this study, the basic mechanisms of persistent infection of RPV have been investigated employing polyclonal antibodies to purified structural proteins of rinderpest virus. The Pi-2 cell line showed the following properties: (1) Do not produce infectious progeny virus particles, (2) The H and F proteins are poorly expressed on the plasma membrane of the Pi-2 cells, (3) Reduced synthesis of M protein, (4) The Pi-2 plasma membrane is less fluid than the acutely infected cells, (5) The nucleocapsids are scattered in the cytoplasm.

Some of these observed properties suggest that the persistent rinderpest virus infection may be associated with the restriction of virus gene and subsequent reduced expression of the glycoproteins at the surface.

In the present study, monoclonal antibodies were used to study the fate of RPV proteins in the Pi-2 cell line in detail. The steady-state levels, rate of synthesis and turn over of various rinderpest virus-specific proteins were studied in detail, employing both mono and polyclonal antibodies. The non-productive persistently infected cell line (Pi-2) was employed in this study. There is a restriction of expression of surface glycoprotiens, H and F and the matrix protein M in Pi-2 cells. Pulse-labelling and immunoprecipitation studies showed that the synthesis of F, and to a lesser extent N, were reduced while that of H protein was undetectable in the unprocessed form. However, very small quantity of H begins to appear during the subsequent chase. The turn over rates of F were different in the two cell types. The kinetics of transport of newly synthesised H protein to the cell-surface in Pi-2 cells were the same as that of acutely infected cells. Since there is a reduction in intracellular synthesis, the amount found on the cell surface was also reduced. This was true for F proteins also. Further, comparison of the cell-surface binding to H protein by different monoclonal antibodies reveals epitopic variation in the H and N protein made in the Pi-2 cells, as revealed by ELISA, although the variation

in N protein epitopes was less. There is reduced intracellular fluorescence in Pi-2 cells with N- and H-monoclonal antibodies, while there is reduction in the cell-surface immune-fluorescence with H-monoclonals, correlating with reduced synthesis and cell-surface expression of the H proteins.

There was a total lack of M protein synthesis in RPV-persistent infection. This may be due either to point mutations in the coding regions of M gene resulting in premature termination of the protein synthesis or to occurrence of point mutations in the 5′ non-coding region which may reduce the ribosome binding or initiation of translation.

References

1. KESARI, K. V. — *Characterization of rinderpest virus and mechanisms of its persistence in Vero cells*, Ph.D Thesis, Indian Institute of Science, Bangalore, India, 1985.
2. ÖRVELL, C. AND NORRBY, E. — *J. Gen. Virol.*, 1980, **50**, 231–245.
3. BARRETT, T. — *Biochem. Soc. Symp.*, 1987, **53**, 25–37.
4. SHESHBERADARAN, H., CHEN, S. N. AND NORRBY, E. — *Virology*, 1983, **128**, 341–353.
5. BHAVANI, K., ANJALI A. KARANDE AND SHAILA, M. S. — *Virus Res.*, 1989, **12**, 331–348.
6. KESARI, K. V. AND SHAILA, M. S. — *Indian J. Biochem. Biophys.*, 1988, **25**, 574–580.

Thesis Abstract (Ph.D.)

Cell walls, wall autolysins and protoplasts from *Microsporum canis* by R. L. Deopurkar.
Research supervisor: G. Ramananda Rao.
Department: Microbiology and Cell Biology.

1. Introduction

The cell wall is the outermost cell structure which comes in direct contact with external environment. In the case of dermatophytes like *Microsporum canis*, it might serve as a barrier to the destruction of the invading fungi by the host defences. Detailed analysis of cell wall, cell-wall-associated enzymes and the involvement of these in apical growth of fungal hyphae are prerequisites towards a better understanding of the basis of pathogenesis.

2. Materials and methods

Microsporum canis strain HM382 used in this study was isolated from clinical lesions[1]. The procedure for the preparation of purified cell walls from *M. canis* was standardised, and the purity was assessed by coomassie blue staining, phase-contrast microscopy and electron microscopy. Detailed chemical analysis of the cell walls was carried out.

Cell-wall autolysis from *M. canis* was studied in detail. Protoplasts were prepared from *M. canis*. Studies were carried out on them to demonstrate their metabolic potential and the ability to regenerate to parental mycelial form.

3. Results and discussion

The cell-wall preparations of *M. canis* were examined under electron microscope. They did not stain with coomassie blue indicating that they are free of cytoplasmic material. The purity of cell-wall preparations was thus established. Cell walls were seen to be consisting of one single layer.

Chemical analysis of cell walls of *M. canis* revealed neutral sugars (about 40–45%), amino sugars (9–10%), proteins (11–14%), lipid (8%) and phosphorous (0.6%) as its constituents. Paper chromatography and gas-liquid chromatography analysis showed glucose and mannose as the only sugars in cell walls of *M. canis*. Our results showed that while glucose was the predominant constituent of the cell walls of *M. canis*, galactose was not present. In the case of fungi belonging to Group V[2] and to which dermatophytes belong, galactose, xylose and fucose are the minor sugars present in cell walls. Amino sugars constitute 9.2% of cell walls of *M. canis* and it appears to be glucosamine. Galactosamine, not detected in the cell walls of *M. canis*, is not a widely reported constitutent of cell wall[3]. As shown in this study, cell walls of *M. canis* do contain significant amount of proteins as in many other fungi. These proteins could be resolved into two fractions on Pharmacia Mono Q HR 5 5 column using 0 to 0.3 M-sodium-chloride gradient.

Cell walls of *M. canis* contained 7.7% lipids. Most of them were neutral lipids and no phospholipid was present. Very little information is available[4–6] regarding types of lipids, nature of fatty acids present in cell walls of fungi. Lipids of cell walls of *M. canis* were investigated in detail. Gas-liquid chromatography analysis revealed that lipids of cell walls of *M. canis* contained fatty acids ranging from C_{12} to C_{20}; nearly 50% of them were saturated fatty acids.

Microorganisms commonly produce enzymes which hydrolyse polymers in their own walls and these are referred to as autolysins. In view of our findings that cell walls of *M. canis* do contain 12.7% (w/w) protein, we investigated in detail autolysins in cell walls of *M. canis*. Purified cell walls of *M. canis* when incubated in buffers released neutral sugars, amino sugars and amino acids. Cell walls boiled with sodium dodecyl sulfate (SDS) failed to do so, clearly indicating the enzymatic nature of the reaction. The nature of the products released is an indication of glucanase, chitinase and protease activities in cell walls of *M. canis*. No information is available regarding wall autolysins of dermatophytes in general and *M. canis* in particular.

Cell-wall autolysins of *M. canis* ceased to act, *in vitro*, even though a large part of cell-wall polymers was still undigested. This is probably due to differential sensitivities of the apical and lateral walls to the action by cell-wall autolysins. Autolysins, first thought solely as a means of degeneration, have excited considerable interest of late as possible factor involved in cell-wall biosynthesis. As first suggested by Bartnicki-Garcia[7] delicate balance between wall synthesis and wall lysis at the apex of growing hypha is of great importance for the growth of hypha. Our current knowledge of cell-wall metabolism is imbalanced as we know much more of the wall synthesis than the wall lysis.

Wall autolysis, in the case of *M. canis*, is significantly affected by pH. Our results show that amongst the enzyme activities monitored glucanase is highly sensitive to pH; chitinase and protease were markedly affected by alkaline pH but not to any significant extent by acidic pH. Wall autolysins of *M. canis* were found to be stable at higher temperature. If one considers wall autolysins as hydrolytic enzymes immobilised in cell-wall polysaccharide matrix, their thermostability is not unexpected. In fact, preexposure of cell walls of *M. canis* to 50°C for 10 minutes resulted in activation of glucanase. The physical alteration, involving disruption of hydrogen bonds, might have increased the accessibility of polysaccharides to enzymatic attack.

Study of effect of metal ions on wall autolysins of *M. canis* revealed interesting findings. Hg^{++} and Fe^{++} inhibited glucanase, chitinase and protease activities of cell walls. Ca^{++} and Cu^{++} inhibited

protease but activated glucanase. Zn^{++} activated protease while inhibiting both glucanase and chitinase. Mn^{++} activated protease and inhibited chitinase. Our results show that glucanase and chitinase in cell walls of *M. canis* were inhibited whenever protease was activated by effector-like metal ions. It is possible that in *M. canis*, coordination between wall synthesis and wall degradation is effected through protease(s) in cell walls. Glucanase, chitinase and protease activities in cell walls of *M. canis* were not inhibited by sulfhydryl-reactive compounds. Cell-wall autolysins of *M. canis* were found to be solubilised during autolysis, and were not found to be under catabolite repression by glucose.

Protoplasts of fungi serve as a model system in studies on cell wall because the synthesis of the cell wall is the prime event during regeneration. Hence protoplasts were prepared from *M. canis* using Novozym 234. The demonstration that each protoplast contains a full set of cytoplasmic organelles, lacks only its cell wall and represents a complete cell is of great significance. The incorporation of radioactive precursors, *viz.*, ^{3}H-thymidine, ^{3}H-uridine and ^{14}C-phenylalanine by regenerating protoplasts of *M. canis* provides evidence for their metabolic potential. The regenerating protoplasts of *M. canis* also incorporated ^{14}C-glucose into alkali-insoluble polysaccharides of the cell walls of *M. canis* and the process was found to be inhibited by 2-deoxyglucose. As shown in this study protoplast will serve as a suitable model system for the study of cell wall synthesis and might prove to be a valuable tool in search of antidermatophytic chemotherapeutic agents having cell-wall synthesis as their target site.

References

1. VIJAYA MANOHAR, RAMANANDA RAO, G. AND SIRSI, M. — *Arogya*, 1977, **3**, 31–40.
2. SAN-BLAS, G. — *Mycopathologia*, 1982, **79**, 159–184.
3. ARONSON, J. M. — In *Biology of conidial fungi*, Vol. 2, 1981 (Cole, G. T. and Kendrick, O., eds), pp 459–507, Academic Press.
4. DYKE, K. G. H. — *Biochim. Biophys. Acta*, 1964, **82**, 374–384
5. LASETER, J. L., WEETE, J. AND WEBER, D. J. — *Phytochemistry*, 1968, **7**, 1177–1181.
6. FISHER, D. J., HOLLOWAY, P. J. AND RICHMOND, D. V. — *J. Gen. Microbiol.*, 1972, **72**, 71–78.
7. BARTNICKI-GARCIA, S. — In *Microbial differentiation* (Ashworth, J. M. and Smith, J. E., eds), 1973, pp 245–267, Cambridge University Press.

Thesis Abstract (Ph.D.)

Immunological and biochemical characterization of protein antigens of *Mycobacterium tuberculosis* $H_{37}R_a$, as recognized by sera from tuberculosis patients by Naishadh N. Desai.
Research supervisor: R. Nayak.
Department: Microbiology and Cell Biology.

1. Introduction

Tuberculosis is a major health hazard in developing countries like India. Availability of new and powerful drug regimens have reduced the mortality rate, but the lack of a suitable diagnostic test and the absence of an effective vaccine still places tuberculosis as a major cause of loss of human lives. Many unique or novel substances reported from mycobacteria have been employed to overcome the above-mentioned difficulties, but were met more with failure than success. Following a different line of thought, the sera from tuberculosis patients were used in the present investigation to characterize the immunogenicity of the proteins of *Mycobacterium tuberculosis* $H_{37}R_a$.

2. Experimental

M. tuberculosis $H_{37}R_a$ was grown on Youmans medium[1] and cells were harvested after mid-log phase by centrifugation. Cell extracts were prepared by grinding the cells in mortar and pestle with glass powder.

ELISA and Western blots were carried out of sera from tuberculosis patients using *M. tuberculosis* cell extract as the antigen. In both the methods, only Tween 20 at suitable concentration was used as the blocking agent. Otherwise, standard procedures were followed[2,3].

The antigens were gel-cut and injected in rabbits to raise antisera against them. Agar-gel precipitation test, immunoelectrophoresis and two-dimensional immunoelectrophoresis were carried out as per standard procedures[4].

Displacement ELISAs were performed by allowing the reaction between different concentrations of the antigen and the appropriate antibody dilution in tubes. These suspensions were transferred to competing antigen-coated plates and further assay was performed as described earlier.

Other mycobacterial species were grown and their extracts prepared in the way similar to that for *M. tuberculosis*.

3. Results and discussion

Antibodies raised by artificial immunization against the *Ra*-cell extract in rabbits reacted with most of the proteins in the extract indicating that artificial immunization leads to a very strong humoral immune response which will not be suitable in distinguishing between antigenic and non-antigenic proteins.

Sera from tuberculosis patients were characterized using conventional immunological techniques and advanced ones like ELISA and immunoblot. Of the 76 sera tested, 45 were having very low antibody titres against the *M. tuberculosis* extract. Amongst the remaining sera giving higher titres, five antigens (designated 1 to 5) were identified using native PAGE-immunoblot technique. On SDS-PAGE-immunoblot, they recognized at least ten different polypeptides ranging in mol wt from

18 to 80 kD. Antigens 1, 2 and 3 were found to be identified by majority of sera, while antigens 4 and 5 were not. Antigens 1 and 2 were selected for further characterization.

The molecular weight determination revealed antigen 1 to be of 65 kD while that of antigen 2 was 36–38 kD. Isoelectric focusing showed that the pIs of antigen 1 and 2 were 6.8 and 7.2, respectively. They were found to contain none or very low amounts of carbohydrates. Mycobacterial extracts are reported to have high amounts of lipids and polysaccharides, which made the purification of these proteins difficult using conventional techniques[5].

Antigen 1 and antigen 2 were band-cut and gel-eluted from non-denaturing polyacrylamide gel. Antibodies were raised against them in rabbits. Immunochemical characterization of these sera was carried out using diverse techniques like immunoelectrophoresis, tandom two-dimensional immunoelectrophoresis and later by ELISA and immunoblot. On initial characterization, both the sera gave more than one precipitin line or arc when tested against the *Ra*-cell extract. On 7.5% native PAGE-immunoblot, anti 65-kD serum identified antigens 1, 2 and 3, while anti 36-kD serum recognized antigens 2, 3 and 5. Similarly, in 10% SDS-PAGE-immunoblot analysis, anti 65-kD serum identified 18 different polypeptides ranging in mol wts from 18 to 80 kD. Anti 36-kD serum identified five polypeptides of mol wt 50, 36.5, 32, 29 and 11.6 kD. Three other mycobacterial species were analysed using these sera, *viz.*, *M. smegmatis*, *M. gordonae* and *M. chelonei*. In each species, a corresponding protein was recognized which confirms the earlier observations that mycobacteria do show strong inter-species cross-reactivity.

Displacement ELISA using these antisera with different mycobacterial extracts showed that the extent of cross-reactivity was much lower being confined only to the respective cross-reactive antigens among these species. The 65-kD protein was not able to displace the 36-kD protein–anti 36-kD serum reaction, confirming that anti 36-kD serum does not recognize the 65-kD protein. It is plausible that the cross-reacting epitopes are present on the 65-kD protein but they are hidden and thereby are not available for anti 36-kD serum to bind. It is argued that the monoclonal sera, unless a large battery of them is employed in an analysis, will not be able to identify cross-reactive epitopes amongst apparently different protein molecules, which, using polyclonal sera, the present study is able to demonstrate.

The 65-kD protein has been reported to share epitopes with diverse molecules like equivalent proteins from many other microbes and GroEL protein of *E. coli*[6]. Displacement ELISA was used to define the cross-reactivity of antigen 1 and antigen 2 with *E. coli* extract and BSA. But the negligible binding observed was thought to be non-specific.

Immunosorbent-anti-65-kD-serum-affinity chromatography was employed to purify the 65-kD protein. But the eluants contained four different polypeptides, the major peak being that of the 36-kD protein as observed on immunoblot. Incubation of the *Ra*-cell extract at 37°C for periods up to 48 h led to the degradation of the 65-kD protein.

There was substantial increase in the quantity of a protein corresponding to antigen 2 as seen on native PAGE. Peptide mapping in the second dimension, using *S. aureus* V8 protease, of the *Ra*-cell extract proteins, after separating them on 10% SDS-PAGE further confirmed that the 65-kD protein gives rise to the 36-kD protein upon degradation.

The presence of antibodies to the 65- and 35-kD proteins was tested in sera from tuberculosis patients. The results differed somewhat from the earlier observations. As the number of sera analysed was limited, this variation was expected.

Antibodies, if raised against those epitopes of the 65- or 36-kD proteins which are unique only to

the pathogenic mycobacteria, can serve as a potential tool for a diagnostic test. Proteins, cross-reactive with the 65- and 36-kD proteins from the pathogenic mycobacteria other than *M. tuberculosis* like the 58-, 29- or 11.6-kD proteins, can be used as markers for studying the prognosis of the disease. A protein of 18 kD has been recognized by more number of sera from tuberculosis patients. In *Ra*-cell extract, it is recognized very strongly by anti-36-kD serum, in fact, more than the homologous antigen itself. This 18-kD protein may be used in cases of tuberculosis as a marker, where the causative agent is *M. tuberculosis*.

References

1. YOUMANS, G. P. AND CARLSON, A. G. — *A. Rev. Tuberc. Pulmonary Dis.*, 1947, **55**, 529–534.
2. CAMPBELL, A. M. — In *Monoclonal antibody technology – The production and characterization of rodent and human hybridomas*, 1984, p. 45. Elsevier.
3. TOWBIN, H., STAEHELIN, T. AND BORDON, J. — *Proc. Natn. Acad. Sci. USA*, 1979, **76**, 4350–4354.
4. HUDSON, L. AND HAY, F. C. — *Practial immunology*, 2nd edn, 1980, Blackwell Scientific.
5. GLENCHUR, H., FOSSIECK, B. E. JR. AND SILVERMAN, M. — *Am. Rev. Respiratory Dis.*, 1966, **93**, 70–77.
6. KAUFMANN, S. H. E. — *Curr. Topics Microbiol. Immunol.*, 1988, **138**, 141–176.

Thesis Abstract (Ph.D.)

Immunotargeting of daunomycin and adriamycin against avian myeloblastosis virus infection

by K. V. R. Dhananjaya.
Research supervisors: A. Antony and G. Ramananda Rao.
Department: Microbiology and Cell Biology.

1. Introduction

Most of the known anticancer agents have been found to be toxic to normal cells. The anthracycline antibiotics daunomycin and adriamycin were found to inhibit several tumour cells *in vitro*[1]. However, these antibiotics were shown to cause acute cardiotoxicity *in vivo*[2]. Liposomes have been shown to be good carriers of drugs as they minimize the toxic effects of encapsulated drug[3]. However, free liposomes are not target-specific. Antibodies raised against specific cell-surface antigens have been coupled to liposomes and used for the targeted delivery of drugs[4]. In the present studies, an attempt was made to explore the possibility of targeting antiviral agents daunomycin and adriamycin encapsulated in immunoliposomes against avian myeloblastosis virus infection in chicks.

2. Experimental

Antibodies against avian myeloblastosis virus envelope glycoprotein gp80 were raised in rabbits and characterized. Immunoliposomes were prepared using phosphatidyl choline, cholesterol and stearylamine in a molar ratio of 51:21:15 and palmitoylated rabbit anti-AMV gp80 as described by Huang *et al*[5]. The drug was encapsulated into immunoliposomes as described by Shen *et al*[6]. Liposomes prepared in this way are unilamellar vesicles with an average size of 300 Å and retained 93% of the

encapsulated drug when incubated in medium containing serum at 37°C for 24 h. AMV-transformed myeloblasts derived from leukaemic chicks and yolk sac cells derived from 13-day-old embryonated chicken eggs were cultured as described earlier.

3. Results and discussion

The effect of daunomycin and adriamycin on AMV-reverse transcriptase and its associated activities has been studied. They inhibited both RNA- and DNA-dependent DNA polymerase activities to 70% at 2 μg concentration. The inhibition was observed irrespective of ribo- or deoxyribonucleic acid templates used in the assay. Time kinetic studies have revealed that ongoing DNA synthesis is also inhibited by the drugs. Kinetic analysis revealed that the inhibition is competitive with respect to the template. The antibiotics were shown to bind to the viral RNA which results in the inhibition of enzyme activity. In addition, the RNase-H and DNA endonuclease activities associated with AMV-reverse transcriptase were inhibited significantly by these antibiotics.

Immunoliposomes were found to bind to polystyrene plates coated with AMV. The binding of immunoliposomes to AMV was analysed by scanning electron microscopy. Quantitative analysis revealed that immunoliposomes bind to virus to a greater extent than free liposomes or nonspecific immunoliposomes. The binding of immunoliposomes to virus-transformed cells was inhibited when the cells were preincubated with homologous antibody. Incubation at low temperature and pretreatment of cells with metabolic inhibitors decreased the uptake of immunoliposomes by virus-transformed cells. The drug encapsulated in immunoliposomes was not significantly taken up by nontarget cells. More drug was delivered into target cells when the drug encapsulated in immunoliposomes was incubated with the cells. The drug encapsulated in immunoliposomes was able to inhibit the RNA synthesis twice more than free drug in the virus-transformed myeloblasts. Pre-treatment of cells with ammonium chloride, reversed the effects of drug encapsulated in immunoliposomes. Colony formation by virus-transformed cells and focus formation by virus-infected yolk sac cells were inhibited significantly by the drug encapsulated in immunoliposomes.

Comparative pharmacokinetics of free drug, drug encapsulated in free liposomes and of drug encapsulated in immunoliposomes in the virus-infected chicks revealed that (i) the drug encapsulated in liposomes was cleared from the plasma slowly, and (ii) the drug encapsulated in immunoliposomes accumulated in the target tissue, the bone marrow, 5 and 8.5 fold more than the drug encapsulated in free liposomes and free drug, respectively. The drug encapsulated in immunoliposomes inactivated the virus and exhibited more chemotherapeutic efficacy as compared to controls when injected up to 24-h post-infection. However, when injected 48-h post-infection the drug encapsulated in immunoliposomes did not offer any protection against the virus infection. There is no detectable antibody response against immunoliposomes in the infected chicks.

The present studies revealed that immunoliposomes are better vehicles for drug delivery than free liposomes. Recent studies have shown that pH-, heat- and target-sensitive immunoliposomes are better carriers of drugs, and may be useful in the chemotherapy of viral infection *in vivo*.

References

1. Di Marco, A. *Cancer Chemotherapy Rep.*, 1975, part 3, 6, 91–106.
2. Von Hoff, D. D., Rozenweig, M. and Slavik, M. *Adv. Pharmacol. Chemotherapy*, 1978, **15**, 1–50.
3. Gregoriadis, G. and Allison, A. C. (eds) *Liposomes in biological systems*, 1980, Wiley.

4. HEATH, T. D., BRAGMAN, K. S., MATTHAY, K. K., LOPEZ-STRANBINGER, G. AND PAPAHADJOPOULOS, D. *Biochem. Soc. Trans*, 1984, **12**, 340–342.

5. HUANG, A., TSAO, Y. S., KENNEL, S. J. AND HUANG, L. *Biochim. Biophys. Acta*, 1982, **716**, 140–150

6. SHEN, D. F., HUANG, A. AND HUANG, L. *Biochim. Biophys. Acta*, 1982, **689**, 31–37.

Thesis Abstract (Ph.D.)

Specificity of L-arabinose-binding protein: A computer modelling approach by Chaitali Mukhopadhyay.
Research supervisor: V. S. R. Rao.
Department: Molecular Biophysics Unit.

1. Introduction

The natural affinity and stereoselectivity of carbohydrate–binding proteins and enzymes toward their substrates have long been a source of much interest. Recently, it has been found that such properties are well manifested by the periplasmic sugar-binding proteins of gram-negative bacteria[1]. These proteins serve as specific receptors in bacterial-active transport and chemotaxis. The function of the proteins and their substrate–binding specificity can be appreciated by studying the modes of binding of substrates and various inhibitors to them. L-arabinose-binding protein (ABP), the first periplasmic sugar-binding protein to have an established primary and tertiary structures has been chosen as a model for this purpose.

The molecular approach to study such biomolecular interaction necessitates a detailed knowledge about the three-dimensional structure of the interacting molecules and their complexes. The available X-ray data of ABP contains the data of the unrefined 2.4-Å resolution study[2]. An attempt was, therefore, made to generate three-dimensional models of ABP-ligand complexes using this low-resolution data by a computer-modelling method. Such studies help in understanding the molecular details of ABP-ligand interactions and also provide a theoretical explanation for the binding affinities of various ligands to the protein.

2. Results and discussion

The modes of binding of α- and β-anomers of L-arabinose to ABP have been studied using the computer modelling method. It has been shown that starting from unrefined 2.4-Å resolution data of the protein, it is possible to fit both the anomers unambiguously in the binding site of ABP[3]. These studies have predicted, in agreement with the 1.7-Å refinement studies[4], that these two anomers bind to ABP in similar ways. The predicted hydrogen-bonding scheme also agrees well with the high-resolution studies. The close agreement between the computer-modelling results and the high-resolution refinement data show that the present method can be effectively used to predict the molecular details of protein-substrate interactions.

The modes of binding of α- and β-anomers of D-galactose, D-fucose and D-glucose have been studied[5]. It is suggested that these sugars preferentially bind in the α-form to ABP, unlike L-Ara

where both α- and β-anomers bind almost equally. The best modes of binding of α- and β-anomers of D-Gal and D-Fuc differ slightly in the nature of the possible hydrogen bonds with the protein. The calculated conformational energies of the complexes suggest that D-Gal is a better inhibitor than D-Fuc and D-Glc, in agreement with kinetic studies. The weak inhibitor D-Glc binds preferentially to one domain of ABP leading to the formation of a weaker complex.

This method was then extended to study the modes of binding of various pento- and hexopyranoses to ABP. The sugars chosen for the study, L-ribose, L-lyxose, D-xylose, L-fructopyranose and L-altrose, differ in orientation and nature of substitution at different ring carbons. The computer-modelling studies suggest that change in orientation of the hydroxyl groups at C-2 and C-3 atoms from equatorial to axial position (as in the case of L-Rib and L-Lyx, respectively) drastically reduces the affinity of the sugars to ABP. An equatorially placed hydroxyl group at C-4 also reduces the affinity of the sugar, but the effect is maximum when a bulky substituent (*e.g.*, CH_2OH) is present on the adjacent C-5 atom. It has also been predicted that sugars with a bulky substituent at C-1 (as in L-fructopyranose) or in the axial position at C-5 (as in L-altrose) may not bind to the protein. These studies also highlight the importance of formation of bidentate hydrogen bonds between ABP and the sugars in forming stable complexes. It has been found that in the cases of moderate or weak inhibitors the possibility of formation of such bidentate hydrogen bonds is less.

In conclusion, the present studies have provided information about (1) the favoured modes of binding of various sugars to ABP, (2) the effect of configuration and substitution on the binding of sugars, and have advanced (3) a theoretical explanation for the relative binding affinities of these sugars to the protein. These studies also show how computer-modelling methods can be used to predict the molecular details of protein-ligand interactions even when only low-resolution X-ray data of the protein are available.

References

1. Boos, W. — *A. Rev. Biochem.*, 1978, **43**, 123–146.
2. Gilliland, G. L. and Quiocho, F. A. — *J. Mol. Biol*, 1981, **146**, 341–362.
3. Mukhopadhyay, C. and Rao, V. S. R. — *Int. J. Biol. Macromol.*, 1988, **10**, 217–226.
4. Quiocho, F. A. and Vyas, N. K. — *Nature*, 1984, **310**, 318.
5. Mukhopadhyay, C. and Rao, V. S. R. — *Int. J. Biol. Macromol.*, 1989, **11**, 194–200.

Thesis Abstract (Ph.D.)

Studies on geometrical aspects of metal coordination by Y. S. Geetha.
Research supervisor: C. Ramakrishnan.
Department: Molecular Biophysics Unit.

1. Introduction

Metal ions play a vital role in a large number of widely differing biological processes and their importance is well known. A large number of physical and spectroscopic methods are available

for studying metal ion environments. Apart from these, a study of the available crystal structures of metal complexes will lead us towards understanding of distortions in metal complexes.

2. Definition of parameters

The first step in such a study is to formulate suitable parameters. The parameters are broadly classified as those connected with the metal (metal-end) and those connected with the ligand (ligand-end). The metal-end parameters are based on the geometry of the complexes, while the ligand-end parameters involve the lone pair orbital directions at the ligand atom.

The parameter l is the coordination bond length and represents the distance between the metal and the ligand atom, the coordination bond angle τ denotes the angle subtended by any two ligand atoms at the metal. The best plane passing through the equatorial atoms is obtained using the least-squares fit method. The parameter Δ is the angle made by the line joining the two axial atoms with the normal to the best plane. δ_M represents the deviation of the metal atom from the best plane. Three parameters, δ_L, δ_α and δ_E, have been defined to characterise the non-coplanarity of the equatorial atoms and distortions from regular geometry (square, triangle, etc.).

Three angular parameters ξ, ζ and θ have been defined at the ligand atom. Depending on the type of the ligand group involved in bonding, a 'ligand plane' has been defined. The lone pair orbital directions are fixed depending on the type of hybridisation of the ligand atom. The parameter ξ is the angle between a lone pair orbital direction and L–X_M direction, where X_M is the foot of the perpendicular drawn from the metal on to the ligand plane and L, the ligand atom. There can be two ξ values when there are two lone pair orbitals. In such cases, the smaller of the two values is used for the analysis and the orbital is designated as the 'associated orbital'. The parameter ζ is the angle made by the M–L direction with the L–X_M direction. This gives the out-of-plane orientation of the M–L direction from the ligand plane. θ is the angle between the associated lone pair orbital direction and the coordination bond.

3. Methods and meterials

A program MCORD was developed in FORTRAN to compute the various parameters defined above. This program requires as input the crystal structure coordination of the involved atoms. The values are grouped under suitable intervals and the distributions plotted as histograms. The ranges, averages and standard deviations of the parameters have been studied. This is a commonly used method to analyse parameters and has been used by our group as well as by different workers[1–7].

The analysis has been carried out using crystal structure data on copper, zinc and sodium complexes. Seventy-five copper complexes with 29 octahedral, 25 square pyramidal, 10 square planar, 11 trigonal bipyramidal geometries, 75 zinc complexes with 28 octahedral, 10 square pyramidal, 7 trigonal bipyramidal and 30 tetrahedral geometries and 31 sodium complexes with 25 in octahedral geometry and 6 in square pyramidal geometry were used for the analysis.

4. Results

Some of the salient features of the analysis are:

(a) There is a distinct break in the Cu–O bond length distribution in octahedral and square pyramidal geometries, with the axial lengths being longer than the equatorial lengths. The distribution of the values is shown in Fig. 1. This feature is not observed in Cu–N as well as zinc, sodium complexes.

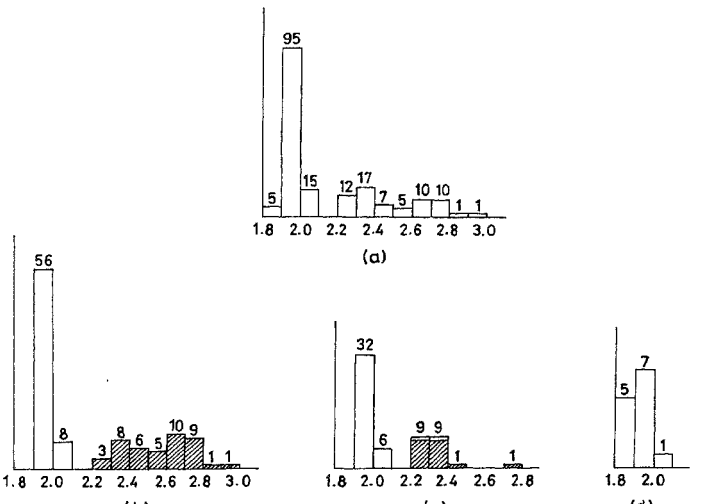

FIG. 1. The distribution of l when oxygen is the ligand atom (in A). (a) General, (b) OCT, (c) SQPY, and (d) SQPL; ▨ axial in b and c.

(b) In the trigonal bipyramidal geometry, it was observed that the axial lengths are shorter than the equatorial lengths in copper complexes and the reverse is true in zince complexes.
(c) It was also observed that the ranges for the parameter l become larger as the coordination number increases from four to six. The bond lengths are short in the case of tetrahedral and square planar geometries and the range is also narrow.
(d) Regarding the coordination bond angles, in the case of copper and zinc complexes, the coordination bond angles (τ) are deviated $\pm 10°$ to $\pm 15°$ from the ideal values. However, generally there is more deviation for the sodium complexes compared to the other metals. The angle subtended at the metal is low when a bidentate ligand is involved in bonding in chelating mode, with one ligand atom in axial and the other in equatorial position.
(e) The ligand-end parameter has a broader range for sodium complexes compared to copper and zinc complexes. It was also observed that the range is broader for θ_0 distribution compared to θ_N distribution in copper and zinc complexes.
(f) It was also observed that there is a strong tendency for the metal atom to lie close to the ligand plane and the $M-L$ direction to lie close to the lone pair orbital.

The ranges that have been obtained for the various parameters can be very useful in (i) any conformational study involving the metal atom and (ii) for detecting any gross distortion in the coordination when exceptional values for the parameters are observed in any new structure.

5. Applications

As a first step towards practical application of the results, a method has been developed to check for the 'suitability' of the ligand atom positions to accommodate a metal. The method requires as input the ranges got from the above analysis.

The procedure comprises two different tests: (i) geometry test, wherein the suitability of ligand atoms for proper coordination is tested as well as the axial and equatorial dispositions (for copper coordination) are also identified, and (ii) parameter test: this decides the proper sequence of the equatorial ligand atoms and checks whether the parameters δ_L, δ_z and δ_E are within the stipulated ranges.

If the above two tests are satisfied, the metal atom is then introduced and moved in a 3D grid. At every grid point, the various parameters are computed and checked against their respective ranges. If all the conditions are satisfied, then the position of the metal is termed 'allowed'. A program MFIX1 has been developed in FORTRAN to carry out the above procedure.

As a test, the method has been applied to a few copper complexes, which have not been included in the analysis. In all the cases, the position of the metal found in the crystal structure was observed to fall within the allowed region obtained in our study. The method can also be used in cases where the metal atom position is unknown.

References

1. RAMAKRISHNAN, C. AND PRASAD, N. *Int. J. Protein Res.*, 1971, **3**, 209–231.
2. MITRA, J. AND RAMAKRISHNAN, C. *Int J Peptide Protein Res.*, 1981, **17**, 401–411
3. LEBIODA, L. *Acta Cryst.*, 1980, **B36**, 271–275.
4. EINSPHAR, H. AND BUGG, C. E. *Acta Cryst.*, 1980, **B36**, 264–271.
5. EINSPHAR, H. AND BUGG, C. E. *Acta Cryst.*, 1981, **B37**, 1044–1052.
6. BAKER, E. N. AND HUBBARD, R. E. *Prog. Biophys. Molec. Biol.*, 1984, **44**, 97.
7. ASHIDA, T., TSUNOGAE, Y., TANAKA, I. AND YAMANE, T. *Acta Cryst.*, 1987, **B43**, 212–218.

Thesis Abstract (Ph.D.)

Synthesis and conformational analysis of analogs of the membrane-active peptides zervamicin IIA and efrapeptin D and peptide containing 1-aminocyclohexane-1-carboxylic acid by M. Sukumar.

Research supervisor: P. Balaram.

Department: Molecular Biophysics Unit.

1. Introduction

This work describes the synthesis and conformational analysis of two 16-residue peptide analogs of the antibiotics zervamicin IIA[1] and efrapeptin D[2] which bear a sequence similarity to the membrane channel forming polypeptide alamethicin. The analog peptides examined in this study are intended

to serve as conformational models for shorter members of the 'peptaibol' family. Detailed structural analysis has been facilitated in both the cases by comparison with shorter peptide fragments. Membrane-modifying activity and aqueous-phase aggregation have also been probed for the zervamicin analog peptides. The stereochemical preferences of the unusual amino acid residue, 1-aminocyclohexane-1-carboxylic acid (Acc^6) and pipecolic acid (Pip) have also been delineated by studies on model synthetic peptides.

2. Synthesis of zervamicin and efrapeptin analogs

The apolar analogs of zervamicin in which all the polar residues in the natural sequence are replaced by apolar residues have been synthesized in order to understand the role of polar side chains in modulating helix association and hence channel-forming activity. The peptides synthesized include the decapeptides R-Trp-Ile-Ala-Aib-Ile-Val-Aib-Leu-Aib-Pro-OMe (R = Boc, Boc-1-10-OMe; R = Ac, Ac-1-10-OMe; R = Dansyl, Dans-1-10-OMe) and the hexadecapeptides R-Trp-Ile-Ala-Aib-Ile-Val-Aib-Leu-Aib-Pro-Ala-Aib-Pro-Aib-Pro-Phe-OMe (R = Boc, Boc-1-16-OMe; R = Ac, Ac-1-16-OMe; R = Dansyl, Dans-1-16-OMe). In the case of efrapeptin analog, pipecolic acid (Pip) and isovaline (Iva) in the natural sequence have been replaced by proline and α-amino-isobutyric acid (Aib), respectively, the sequence of the synthetic peptide being Boc-Pro-Aib-Pro-Aib-Aib-Leu-β-Ala-Gly-Aib-Aib-Pro-Aib-Gly-Leu-Aib-Aib-OMe. All the peptides have been synthesized by solution-phase procedures and were thoroughly characterized by NMR and amino-acid analysis.

3. Conformational analysis and membrane-modifying activity

The solution conformations of Boc-1-10-OMe, Boc-1-16-OMe, efrapeptin analogs and its fragments have been examined by ^1H NMR methods which permit an assessment of the degree of solvent exposure of peptide NH groups and allow characterization of spatially proximate sets of protons *via* the observation of nuclear Overhauser effects (NOEs). High-resolution X-ray structures of one of the zervamicin analogs (Boc-1-16-OMe) and its N-terminal decapeptide have been determined rendering a comparison of structures in the solution and solid states possible[3-5].

The NMR data on Boc-1-10-OMe is consistent with a helical conformation throughout its length in $CDCL_3$ solution, stabilized by either $4 \rightarrow 1$ hydrogen bonds (3_{10}-helix) or mixed $4 \rightarrow 1$ and $5 \rightarrow 1$ hydrogen bonds ($3_{10}/\alpha$-helix). However, a structural transition has been observed on going to strongly hydrogen-bonding solvents like dimethylsulfoxide that involves a partial disruption of the helix at the N-terminus. The conformation of the decapeptide in the solid state (mono- and triclinic polymorphs) is essentially similar to that observed in chloroform solutions. A transition in the helix type from a predominantly α-helical conformation in the triclinic form to a largely 3_{10}-helical structure in the monoclinic form is observed in the solid state[5].

Hydrogen-bonding studies on Boc-1-16-OMe suggest a helical conformation in $CDCL_3$, while on going to DMSO, a structural transition analogous to that observed in the decapeptide has been noticed (Fig. 1). The observed pattern of hydrogen bonding and NOEs is consistent with incorporation of all three Pro residues into the helix. In the solid state the molecule winds into a continuous helix with characteristics of a 3_{10}-helix, α-helix and β-bend ribbon[4]. A significant bend in the helix occurs at residue Pro (10).

The activities of the various zervamicin analogs were compared using two assay systems: i) uncoupling of oxidative phosphorylation, and ii) transport of Ca^{2+} across liposomal membranes. The order of activity obtained from the two assays is the same leading to the following conclusions: 1) The shorter peptides are more active than the longer ones; 2) The acetyl-protected peptides are

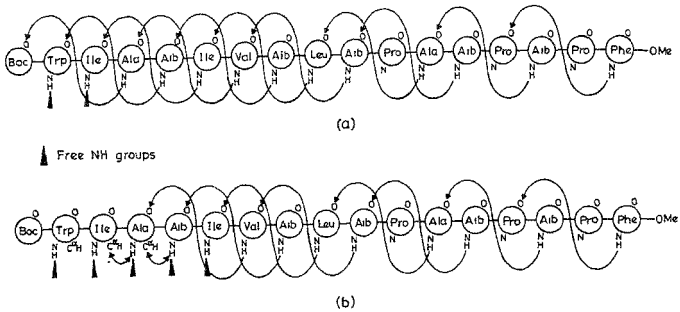

FIG. 1. Proposed intramolecular hydrogen-bonding schemes for Boc-1-16-OMe in a) $CDCL_3$, and b) DMSO-d_6.

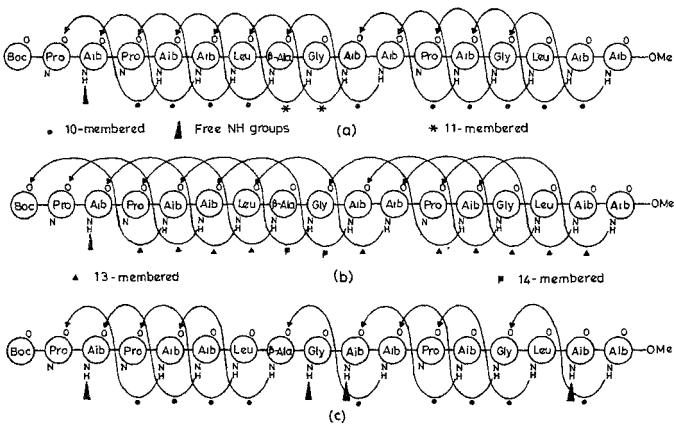

FIG. 2. Proposed intramolecular hydrogen-bonding schemes for efrapeptin analog peptide in $CDCL_3$ (a,b) and DMSO (c).

more active than the Boc-protected ones suggesting a role for the acetyl-blocking group found in natural sequences.

The 16-residue efrapeptin analog has a predominantly helical structure with some possible distortions from the ideal helix, in order to accommodate the additional tetrahedral carbon atom of β-alanine. However, the peptide has a different conformation in DMSO, the two 11-membered H-bonds being absent in this solvent (Fig. 2). This difference in conformation in the two solvents

might be relevant in explaining the unique biological activity of efrapeptin D. The kind of structural transition observed in the case of the 16-residue analog peptide has also been observed in the case of smaller fragments of the analog, suggesting that short-range interactions predominantly dictate the conformational features of the efrapeptin analog. Based on the conformational studies on Pip-containing peptides, the efrapeptin analog peptides and theoretical studies of the pipecolyl residue, possible conformations for natural efrapeptin D have been suggested in solvent-like chloroform and dimethylsulfoxide.

4. Studies on 1-aminocyclohexane-1-caroxylic acid containing peptides

NMR and X-ray studies on model peptides incorporating Acc^6 establish that this residue is compelled to adopt conformations in the $3_{10}/\alpha$-helical regions of ϕ, ψ space[6-8]. The solution conformations of all these peptides are similar to those observed in the solid state and establish the ability of Acc^6 residues to impart stereochemical rigidity to the peptide backbone. A chemotactic peptide analog For-Met-Acc^6-Phe-OMe, incorporating Acc^6 in position 2 of the parent peptide, has been shown to be ~ 78 times more active than the parent peptide[9] suggesting that the peptide-receptor interactions involving residue 2 are an important determinant of the biological activity.

References

1. RINEHART, K. L., GAUDIOSO, L. A., MOORE, M. L., PANDEY, R. C., COOK, J. C., BARBER, M., SEDGWICK, R. D., BORDOLI, R. S., TYLER, A. N. AND GREEN, B. N. — *J. Am. Chem. Soc.*, 1981, **103**, 6517–6520.
2. BULLOUGH, D. A., JACKSON, G. G., HENDERSEN, P. J. F., COTTEE, F. H., BEECHEY, R. B. AND LINNETT, P. E. — *Biochem. Inter.*, 1982, **4**, 543–549.
3. KARLE, I. L., SUKUMAR, M. AND BALARAM, P. — *Proc. Natn. Acad. Sci. USA*, 1986, **83**, 9284–9288.
4. KARLE, I. L., FLIPPEN-ANDERSON, J., SUKUMAR, M. AND BALARAM, P. — *Proc. Natn. Acad. Sci. USA*, 1987, **84**, 5087–5091.
5. KARLE, I. L., FLIPPEN-ANDERSON, J., SUKUMAR, M. AND BALARAM, P. — *Int. J. Peptide Protein Res.*, 1988, **31**, 567–576.
6. BARDI, R., PIAZZESI, A. M., TONIOLO, C., SUKUMAR, M., RAJ, P. A. AND BALARAM, P. — *Int. J. Peptide Protein Res.*, 1985, **25**, 628–639.
7. PAUL, P. K. C., SUKUMAR, M., BARDI, R., PIAZZESI, A. M., VALLE, G., TONIOLO, C. AND BALARAM, P. — *J. Am. Chem. Soc.*, 1986, **108**, 6363–6370.
8. VALLE, G., CRISMA, M., TONIOLO, C., SEN, N., SUKUMAR, M. AND BALARAM, P. — *J. Chem. Soc. Perkin Trans., II*, 1988, 393–398.
9. SUKUMAR, M., RAJ, P. A., BALARAM, P. AND BECKER, E. L. — *Biochem. Biophys. Res. Commun.*, 1985, **128**, 339–344.

Thesis Abstract (Ph.D.)

X-ray Diffraction and theoretical studies on DNA and ligand-DNA interaction by M. Sundaramoorthy.
Research supervisor: V. Sasisekharan.
Department: Molecular Biophysics Unit.

1. Introduction

Natural DNA exhibits three polymorphic forms A, B and C. NaDNA gives C, A and paracrystalline B[1] forms and LiDNA shows C, crystalline B and paracrystalline B forms[2] depending upon the salt concentration and relative humidity. The helical parameters of A and B forms were believed to be unique. However, it has been observed that C form has a variety of helical parameters[3]. The conformational flexibility of DNA[4], smooth transitions from B to C in LiDNA fibres and microheterogeneity in C form suggest that such a microheterogeneity is possible in B form also. Though it was observed in a few studies, it was not characterised in fibres under ambient conditions like alkali salt and relative humidity. The present study has been carried out to investigate polymorphism in LiDNA and microheterogeneity in B-DNA as a function of LiCl concentration and relative humidity.

Oligopeptides like Netropsine (Nt) and Distamycin A (Dst A) bind to AT-rich sequences of B-DNA in the minor groove non-intercalatively[4]. In order to understand the factors involved in the binding of this class of ligands, crystallographic and theoretical modelling studies were carried out for an analogue of Dst A.

2. Materials and methods

Calf-thymus DNA was used to carry out the fibre-diffraction studies. The concentration of LiCl was controlled in the fibres by dialysis[5]. A precession camera was used to record the diffraction patterns at different relative humidities.

A new method was developed for this purpose as the earlier one using a flat-plate camera has the disadvantage of recording a distorted image of the reciprocal lattice. It also does not record the meridional and near-meridional reflections. The precession method eliminates both these drawbacks and this was proved both theoretically and experimentally using the 'rotation-precession' method for single crystal. The measurements and calculations are made easier and accurate in this method.

The crystal structure of pyrrole-β-alanine, an intermediate of a Dst-A-analogue PAP was solved using direct methods and refined by structure-factor least-squares procedure. The interaction studies of the analogue, a dimer of this molecule with end groups similar to those of Dst A, were carried out by energy minimisation technique.

3. Results

A typical B pattern with Li^+/phosphate = 1.6 at 40% relative humidity recorded using the precession camera was found to have the following helical parameters: Pitch = 32.98 Å, Unit height = 3.396 Å and no. of basepairs/turn = 9.72 which are different from the values of the earlier studies. Similarly the diffraction patterns recorded at different relative humidities for various salt concentrations showed a variety of n values deviating from 10 of the B-helix.

The present study also shows that low-salt LiDNA fibres exhibit two polymorphs C and paracrystalline B at low- and high-relative humidities. On the other hand, high-salt fibres show C, crystalline B and paracrystalline B forms at low, moderate and high relative humidities, respectively. The transitions from one polymorph to the other depends on the salt concentration. The transition points shift towards the lower side of the relative humidity scale as the salt increases, reaches a critical concentration and move upwards with increase in the concentration of the salt.

The crystal structure of pyrrole-β-alanine was refined to an R value of 4.4%. The molecule assumes a curved backbone structure with amide groups lying on the concave side. These are the important requirements for the ligand to bind non-intercalatively in the minor groove and the NH groups can form H bonds with the base atoms. The energy minimisation studies of the dimer of this molecule PAP, an analogue of Dst A, with various representative sequences of B-DNA show the following results.

(i) PAP binds to DNA in two orientations with guanidium group pointing up and down equally well.
(ii) The drug shows specificity to AT sequences. The order of stability of interaction is $(dA)_6$, $(dT)_6$, $(dA\text{-}dT)_3$, EcoRI, *i.e.*, d(GAATTC). d(CTTAAG) and $(dG\text{-}dC)_3$.
(iii) All the forces of interaction van der Waals, electrostatic and hydrogen bond contribute to the stability of the complexes.

4. Discussion

The variety of n values different from 10 obtained for B-DNA for different salt concentrations and relative humidities suggests that B-DNA need not be ten-fold integral helix always. It can have a number of microheterogeneous structures with n deviating from 10. Also, the structural transitions in the fibres are analogous to those found in NaDNA fibres. High-salt LiDNA fibres undergo reversible C → crystalline B → paracrystalline B transitions as a function of relative humidity. NaDNA fibres undergo C → A(crystalline) → paracrystalline B transitions[6].

The results of the drug-DNA interaction studies support the findings of earlier physico-chemical studies on distamycin and its analogues with DNA[7]. The ligand should have curved backbone structure isohelical to B-DNA to fit snugly in the minor groove and the NH groups are essential to form hydrogen bonds with base atoms.

References

1. Fuller, W., Wilkins, M. H. F., Wilson, H. R. and Hamilton, L. D. — *J. Mol. Biol.*, 1965, **12**, 60–80.
2. Langridge, R., Wilson, H. R., Hooper, C. W., Wilkins, M. H. F. and Hamilton, L. D. — *J. Mol. Biol.*, 1960, **2**, 19–37.
3. Marvin, D. A., Spencer, M., Wilkins, M. H. F. and Hamilton, L. D. — *J. Mol. Biol.*, 1961, **3**, 547–565.
4. Zimmer, C. and Wahnert, U. — *Prog. Biophys. Molec. Biol.*, 1986, **47**, 31–112.
5. Parrack, P. K., Dutta, S. and Sasisekharan, V. — *J. Biomol. Struct. Dynam.*, 1984, **2**, 149–157.

6. RHODES, N. J., MAHENDRASINGHAM, A., PIGRAM, W. J., FULLER, W., BRAMS, J., VERGENE, J. AND WARREN, R. A. J. *Nature*, 1982, **296**, 267–269.

7. DASGUPTA, D., PARRACK, P. K. AND SASISEKHARAN, V. *Biochemistry*, 1987, **26**, 6381–6386.

Thesis Abstract (Ph.D.)

Crystal structure of the low-humidity form of tetragonal hen egg–white lysozyme by R. Kodandapani.
Research supervisor: M. Vijayan.
Department: Molecular Biophysics Unit.

1. Introduction

Water plays an important role in biological systems and understandably, hydration of proteins and its effect on their structure and action are topics of considerable current interest. High-resolution X-ray analysis of protein crystals appears to indicate that each protein is endowed with a characteristic hydration shell which is substantially conserved with respect to species variation and environmental differences [1,2]. The nature and the extent of the possible changes in the hydration shell, and their effects on protein structure and function have not, however, been examined in detail so far. In this context, water-mediated transformations, being studied in this laboratory[3,4], appear to provide a useful handle for exploring possible changes in hydration and the resultant perturbations in protein structure. Such transformations, which are reversible and typically occur at a relative humidity of around 90%, are accompanied by abrupt changes in unit cell dimensions, diffraction pattern and solvent content. It appeared that these changes cannot be explained exclusively on the basis of simple shrinkage due to loss of solvent. *A priori*, the changes could have resulted from changes in molecular packing, molecular conformation or hydration, or most probably, a combination of the three. The contributions of these three elements, can be comprehensively elucidated only through the high-resolution X-ray analyses of low-humidity forms and the comparison of the resulting structures with those of the corresponding native crystals. As a first step in an effort in this direction, the low-humidity form of the well-known tetragonal lysozyme[5,6] has been taken up.

2. Data collection and processing

Data at 88% r.h. from low-humidity crystals up to a resolution of 2.1 Å were collected using oscillation photography followed by computer-controlled microdensitometry. The data were processed, scaled and post-refined using programmes originally developed by Rossmann[7]. To collect the entire data, 21 crystals and 46 film packs were used. A total of 68244 reflection intensities were measured from which the intensities of 7127 unique reflections were derived. The unique data set contained 9 overloaded reflections. The intensities of these reflections were taken from a scaled diffractometer data set collected up to a resolution of 3.34 Å. This data set was also used as a check on the reliability of the photographic data set.

3. Structure analysis

Exploratory investigations using different Fourier syntheses based on native phases and rotation function calculations indicated that the transformations were not accompanied by major structural changes. It appeared that the structure of the native crystals as such could serve as a good starting point for the refinement of the low-humidity form. The fractional coordinates of the protein atoms in the native crystals, supplied by Phillips and co-workers, were used without modifications in the starting model. The Hendrickson-Konnert-restrained least-squares programme[8], as modified by Eleanor Dodson to incorporate Agarwal's FFT method[9], was used for structure refinement on a DEC 1090 system. The temperature factors were not restrained during refinement. Altogether 140 cycles of refinement calculations were carried out. During the course of the refinement, several Fourier maps, including an 'omit' type map, were examined to correct the model and also to locate water molecules. The refinement converged at $R = 0.1623$ for 6269 reflections with $I > 2\sigma(I)$. The final model contains 1001 protein and 157 water oxygen atoms. The Luzzati plot indicates the average coordinate error to be 0.15 Å.

4. Results and discussion

Among the four helical stretches stabilized predominantly by $5 \rightarrow 1$ hydrogen bonds, comprising residues 15–25, 25–36, 88–101 and 109–115, the first three have helical parameters close to those for an α-helix. The short stretches (80–84 and 120–124) containing $4 \rightarrow 1$ hydrogen bonds have mean helical parameters intermediated between those for a 3_{10} helix and an α-helix. The β-structure and α-turns are additionally stabilized by extensive side chain–main chain and side chain–side chain interactions. The protein molecule contains two inverse γ-turns, an α-turn and a β-bulge. One hundred and twenty-one water molecules surround each protein molecule, and nearly half of them have multiple interactions with the protein. There are 15 well-defined ($B = 30$) water molecules having three or more interactions with the protein and many of them are involved in helping to hold different regions of the molecule together. Some water molecules contribute to the stability of β-turns. Side chains with multiple hydrogen-bonding centres, and regions between a short hydrophilic side chain and the main chain NH or CO group of the same or a neighbouring residue appear to provide specific sites for hydration.

The protein molecule as a whole moves slightly in the low-humidity form from its position in the native crystals. The main-chain conformation is almost the same in the two structures. Larger differences occur in the side chains. Some side chains move in concert such that the interactions between them remain unchanged. Interestingly, the side chain of 62 Trp and many atoms in the loop move substantially during the transformation. These regions are known to move during inhibitor binding also. Other active site residues that move during the transformation include 37 Asn and 44 Asn. The number of water molecules in the first hydration shell, which as a whole tends to move along with the protein molecule, remains nearly the same in the two structures. Significant differences however exist in the location of molecules in the shell. Even on a liberal criterion, only less than two thirds of the water molecules are equivalent in the two structures. Understandably, the water molecules least affected by the transformation are multiply and strongly bound ones. In the case of singly or doubly bound water molecules, the effect is higher when they are bound to side chains.

References

1. Blake, C. C. F., Pulford, W. C. A. and Artymiuk, P. J. *J. Mol. Biol.*, 1983, **167**, 693–723.

2. BAKER, E. N. AND HUBBARD, R. E.	*Prog. Biophys. Mol. Biol.*, 1984, **44**, 97–179.
3. SALUNKE, D. M., VEERAPANDIAN, B. AND VIJAYAN, M.	*Curr Sci*, 1984, **53**, 231–235.
4. SALUNKE, D. M., VEERAPANDIAN, B., KODANDAPANI, R. AND VIJAYAN, M.	*Acta Cryst.*, 1985, **B41**, 431–436.
5. BLAKE, C. C. F., KOENIG, D. F., MAIR, G. A., NORTH, A. C. T., PHILLIPS, D. C. AND SARMA, V. R.	*Nature*, 1985, **206**, 757–761.
6. IMOTO, T., JOHNSON, L. N., NORTH, A. C. T., PHILLIPS, D. C. AND RUPLEY, J. A.	In *The enzymes*, (P. D. Boyer, ed) Vol 7, 1972, pp 665–808, Academic Press.
7. ROSSMANN, M. G.	*Methods in enzymology*, Vol. 14, 1985, pp 237–280.
8. HENDRICKSON, W. A. AND KONNERT, J. H.	In *Computing in crystallography* (R. Diamond, S. Ramaseshan and K. Venkatesan, eds), 1980, pp 13.01–13.26, Indian Academy of Sciences, Bangalore.
9. AGARWAL, R. C.	*Acta Cryst.*, 1978, **A34**, 791–809.

Thesis Abstract (Ph.D.)

_B_-to-_Z_ transitions in synthetic polynucleotides by Latha P. Kadalayil.
Research supervisor: Samir K. Brahmachari.
Department: Molecular Biophysics Unit.

1. Introduction

The double helical structure of DNA proposed by Watson and Crick[1], which paved the way for the development of molecular biology, did not emphasize the importance of the sequence dependence of conformation. As a result, the DNA molecule was considered to be relatively monotonous in structural terms. However, the last decade has witnessed dramatic changes in the earlier concepts through both theoretical studies on polynucleotide conformation[2–4] and X-ray crystallographic studies of polynucleotides[5] and oligonucleotides[6–8]. Further, the availability of the structure of left-handed _Z_-DNA at atomic resolution[6,7] prompted us to look in detail into the factors controlling structural transitions involving change in handedness, as the exact mechanism of such transitions was very poorly understood. Hence, we addressed ourselves the following questions in order to have a better perspective of the _B_ (right-handed) to _Z_ (left-handed) transitions in DNA in solution and its biological relevance.

1. Is the $B \rightleftharpoons Z$ transition thermodynamically controlled?
2. Are the $B \rightleftharpoons Z$ transitions induced by different environmental factors kinetically distinguishable?
3. What is the role of counterions and water structure in bringing about the $B \rightleftharpoons Z$ transitions?
4. How do modifications of the bases affect the $B \rightleftharpoons Z$ transitions?
5. Do only alternating CG sequences favour $B \rightleftharpoons Z$ transitions?
6. What is the exact requirement of base sequence for the formation of _Z_-DNA?
7. What is the nature of interaction of such sequences with proteins?

To have an in-depth understanding of the above-mentioned aspects of $B \rightleftharpoons Z$ transitions, the

physicochemical studies of synthetic polynucleotides and oligodeoxynucleotides containing alternating pyrimidine-purine sequences were undertaken, the results of which are described below.

2. Experimental

The oligodeoxynucleotides studied in this report were synthesized manually using phosphoramidite method according to published procedures[9]. The purification was carried out using reversed-phase and anion-exchange HPLC methods[10,11]. Polynucleotides (Pharmacia-PL Biochemicals) were used after extensive purification procedures to eliminate the multivalent ion impurities that may be present. The concentration of the oligonucleotides and polynucleotides was determined from their extinction coefficients at appropriate wavelengths.

CD and/or UV spectroscopic studies were employed for monitoring the $B \rightleftharpoons Z$ transitions. CD studies were carried out using a Jasco J 20 automatic-recording spectropolarimeter. UV studies were carried out using a Beckman DU8B spectrophotometer attached with Tm and kinetic accessory.

3. Results and discussion

The formation of Z-DNA has been found to be favoured mostly by alternating purine-pyrimidine sequences[12,13]. Therefore we have taken up such sequences for our studies.

3.1 *$B \rightleftharpoons Z$ transition in poly(dG-dC): A case of non-isoenthalpic change*

The reversible transition of poly(dG-dC) in high salt was thought to be temperature independent[14]. It is for the first time we showed that a Z-to-*B* transition in poly(dG-dC) in 60% ethanol could be achieved with increase in temperature and the process is non-isoenthalpic[15]. Transition temperature is sensitive to cation concentration, thus making it biologically significant. Now, several workers have shown that temperature-dependent *B*-to-*Z* transition could take place under a variety of conditions.

3.2 *Kinetic studies of B-to-Z transitions in poly(dG-dC) and poly(dG-Me^5 dC)*

The $B \rightleftharpoons Z$ transition in polynucleotides has been shown to be promoted by several factors like cations, ligands and solvent changes[12,13]. A comparative study of the kinetics of *B*-to-*Z* transitions in the presence of various factors has been carried out to check whether these transitions are kinetically distinguishable. Such an approach has not been adopted by earlier researchers. Our results show that the $MgCl_2$ and hexamine-cobalt-chloride (HCC)-induced transitions like the one mediated by NaCl were found to be intramolecular in nature. The transition that took place in the presence of ethanol was not found to be so. The rate of the ethanol-induced *B*-to-*Z* transition was found to depend on the concentration of the polynucleotide, *i.e.*, the transition became slower with increasing concentrations of the polymer. This is an indication of an intermolecular process in which an aggregated species may form an intermediate between the *B*- and *Z*-forms. Interestingly, in spite of the requirement of less-stringent conditions for the $B \rightleftharpoons Z$ transitions of poly(dG-Me^5 dC), its kinetics were found to be slower than those of poly(dG-dC). The universal nature of the slow kinetics can be explained in terms of the rearrangement of water molecules around the DNA molecules while going from *B*- to *Z*-form.

3.3 *Antisynergistic effect of phosphate ions and ethidium bromide in the presence of Z-inducing agents*

$Co(NH_3)_6Cl_3$(HCC)-induced $B \rightarrow Z$ transition of poly(dG-dC) in the presence of phosphate ion was studied. The results indicate that phosphate ions present in the medium had an inhibitory effect on the $B \rightarrow Z$ transition. This must be due to the non-availability of the HCC molecules that are necessary for the stabilization of Z-DNA, as the binding sites of these molecules are now divided between free phosphate ions of the medium and those of the DNA backbone. This in turn is a direct evidence for the involvement of binding of HCC to phosphate groups of DNA in the stabilization of Z-conformation.

Destabilizing effect of ethidium bromide on the Z-form of poly(dG-dC), poly(dG-Me^5dC) and brominated poly(dG-dC) was investigated. It was observed that ethidium bromide is less efficient in counteracting the effect of chemical modifications than that of ethanol, in the unmodified polymer. The increased hydrophobicity in the case of poly(dG-Me^5dC) and steric hindrance created by the bulky bromine atoms in the case of the brominated analogue may be responsible for this phenomenon.

3.4 *Low-salt $B \rightleftharpoons Z$ transition in poly(dG-Me^5dC): Effect of ion and temperature: Role of DNA methylation*

The occurrence of a B-to-Z transition with decreasing monovalent cation concentration has been reported for the first time from our laboratory[16]. To elaborate, it was found that poly(dG-Me^5dC) underwent a novel $Z \rightleftharpoons B \rightleftharpoons Z$ transition on increasing the Na^+ concentration. We also observed that Cs^+ and Li^+ ions, in spite of their differences in charge density and water of hydration stabilize this low-salt Z-form in a way similar to Na^+ ion. Anions like perchlorate, which are known to have solvent-structure-breaking property, were found to affect the low-salt B-to-Z transition differently from the chloride ions. Low-salt Z-conformation was destabilized by ethidium bromide like the high-salt Z-form. It was possible to distinguish the low-salt Z-to-B transition from the high salt one by kinetic studies which suggest a plausible difference in the mechanism for these two transitions. Studies with Mg^{2+} ion indicate the possibility of a Z(II)-type conformation for poly(dG-Me^5dC) in low-salt condition. Both low- and high-salt Z-forms of poly(dG-Me^5dC) have been found to be more stabilized than the B-form at higher temperatures. The inter-relationship between the temperature and counterion puts these transitions at fixed domains as indicated by the phase diagram. The possibility of multivalent ion contamination that may be responsible for the Z-form has been ruled out by performing the experiments with samples subjected to extensive purification methods.

These findings suggest that other than water-structure specific ion binding may also be responsible for stabilizing left-handed Z-DNA conformation.

It is interesting to note that the same factor, *i.e.*, Na^+, which favours a structural transition up to a critical concentration, can reverse the effect at a higher concentration. Hence, any event that demands a Z- to B-transition can be brought about and reversed by the same Na^+. Thus, Na^+ can serve as an autoregulator for a Z- to B-transition of the DNA template containing alternating CG sequences. This effect is observed only when cytosine residues are methylated. Thus, it is tempting to suggest that methylation in conjunction with fluctuation in Na^+ concentration in millimolar level may bring about a reversible B- to Z-transition in small stretches of alternating CG sequences in natural DNA. These stretches could probably then serve as sites for regulation.

Several deoxyoligomers with alternating purine-pyrimidine sequences (having both A-T and G-C base pairs) have been shown to adopt the Z-structure in the solid state. However, in solution, Z-form is favoured only when some of the bases in these sequences are covalently modified. Furthermore, the exact requirement of sequence or chain length for an oligonucleotide containing all four bases

for *B*- to *Z*-transition to occur is not known. With this in view two decadeoxynucleotides d(CGTACGTACG) and d(CGTGCGCACG) have been synthesized by phosphoramidite method and spectroscopic studies have been carried out. Melting studies of these sequences showed that these two decamers existed in duplex form at room temperature. NaCl and HCC titration indicated that both these sequences did not undergo $B \rightarrow Z$ transition even at concentrations one order higher than that required for poly(dG-dC). On comparison with the crystal structures of *Z*-form, it appears that a continuous stretch of CG residues is necessary for a facile $B \rightarrow Z$ transition to take place in solution even for a GC-rich sequence.

References

1. WATSON, J. D. AND CRICK, F. H. C. — A structure for deoxyribose nucleic acid, *Nature*, 1953, **171**, 737–738.
2. SASISEKHARAN, V. — Conformation of polynucleotides, *The Jerusalem Symposia on Quantum Chemistry and Biochemistry*, 1973, Vol. 5, pp 247–260, Academic Press, Jerusalem.
3. SASISEKHARAN, V., BANSAL, M., BRAHMACHARI, S. K. AND GUPTA, G — Conformational flexibility of DNA: A theoretical formalism, *Proceedings of the Second SUNYA Conversation in the Discipline of Biomolecular Stereodynamics*, 1981, Vol. 1, p 123, Adenine Press.
4. SASISEKHARAN, V. — Left-handed DNA duplexes, *Cold Spring Harbor Symposia on Quantitative Biology*, 1983, Vol. 47, pp 45–52.
5. ARNOTT, S., CHANDRASEKARAN, R., BIRDSALL, D. L., LESLIE, A. G. W. AND RATLIFF, R. L. — Left-handed DNA helices, *Nature*, 1980, **283**, 743–745.
6. WANG, A. H. -J., QUIGLEY, G. J., KOLPAK, F. J., CRAWFORD, J. L., VAN BOOM, J. H., VAN DER MAREL, G. A. AND RICH, A. — Molecular structure of a left-handed double helical DNA fragment at atomic resolution, *Nature*, 1977, **282**, 680–686.
7. DREW, H., TAKANO, T., TANAKA, S., ITAKURA, K. AND DICKERSON, R. E. — High-salt d(CpGpCpG). A left-handed Z′ DNA double helix, *Nature*, 1980, **286**, 567–573.
8. DREW, H. R., WING, T., TAKANO, T., BROKA, C., TANAKA, K., ITAKURA, K. AND DICKERSON, R. E. — Structure of a *B*-DNA dodecamer: Conformation and dynamics, *Proc. Natn. Acad. Sci.*, 1981, **78**, 2179.
9. BANNWARTH, W. — *Laboratory protocol*, 1984, Personal communication.
10. MAJUMDER, K., LATHA, P. K. AND BRAHMACHARI, S. K. — Use of volatile buffers at ambient temperature: Versatile approach to the purification of self-complementary synthetic deoxyoligonucleotides by reversed-phase high-performance liquid chromatography, *J. Chromatogr.*, 1986, **355**, 328–334.
11. MAJUMDER, K., LATHA, P. K. AND BRAHMACHARI, S. K. — Synthesis and purification of oligodeoxyribonucleotides: A modified approach, *Curr. Sci.*, 1987, **56**, 693–697.
12. RICH, A., NORDHEIM, A. AND WANG, A. H. -J. — Chemistry and biology of left-handed *Z*-DNA, *A. Rev. Biochem.*, 1984, **53**, 791–846.
13. LATHA, P. K. AND BRAHMACHARI, S. K. — *B*- to *Z*-transitions in DNA and their biological implications, *J. Sci. Ind. Res.*, 1986, **45**, 521–533.
14. POHL, F. M. AND JOVIN, T. M. — Salt-induced co-operative conformational change of a synthetic DNA: Equilibrium and kinetic studies with poly(dG-dC), *J. Mol. Biol.*, 1972, **62**, 375–396.

15 LATHA, P. K., MAJUMDER, K. AND BRAHMACHARI, S. K. Temperature dependent $Z \rightleftharpoons B$ transitions in poly(dG-dC), *Curr. Sci.*, 1983, **52**, 907–910.

16. LATHA, P. K. AND BRAHMACHARI, S. K. A novel structural transition in poly(dG-Me^{5}dC) $Z \rightleftharpoons B \rightleftharpoons Z$, *FEBS Lett.*, 1985, **182**, 315–318.

Thesis Abstract (Ph.D.)

Studies on a ribosome-inactivating protein: Mechanism of inhibition of protein synthesis by gelonin by M. P. Ramprasad.
Research supervisor: A. Surolia.
Department: Molecular Biophysics Unit.

1. Introduction

Ribosome-inactivating proteins (RIPs) are proteins that inactivate heterologous eukaryotic ribosomes in a catalytic manner[1]. Specifically, they inactivate the 60S-ribosomal subunit and render them incapable of binding the elongation factor 2 and thus arrest protein synthesis. RIPs, which are found exclusively in plants, are classified into two types depending on the presence or absence of a linked carbohydrate-binding protein. RIPs type 2 were the first to be discovered and consist of two polypeptide chains: an *A* chain and a *B* chain linked together by a disulfide bond. The *B* subunit is involved in the interaction of the toxin with the sugar moiety of cell-surface receptors, whereas the *A* chain inactivates the 60S-ribosomal subunit. Some examples are ricin, abrin, modeccin, etc. The RIPs type 1 which are more widely distributed in the plant kingdom have only a single polypeptide chain of mol wt 30,000 that resembles the *A* chain of RIPs type 2 in its action, *e.g.*, pokeweed antiviral protein, saporin, dianthins, gelonin, etc. The exact *in vivo* function of RIPs is not known but it is thought that they may be involved in regulation of protein synthesis, in reducing the frequency of spontaneous successful grafts in nature or act as antifungal agents. The fungal RIPs like α-sarcin and mitogillin have a mol wt of 17,000 daltons and their detailed subribosomal mechanism of action was the first to be worked out. α-Sarcin catalyses the inactivation of the 60S-ribosomal subunit by specifically cleaving a 488-nucleotide fragment from the 3′ end of 28S rRNA in rat liver polysomes. The mode of action of ricin, the best studied RIP so far, was very recently established after considerable efforts[2]. It acts adjacent to the α-sarcin site and stoichiometrically removes a single adenine base from the ribosome by an N-glycosidase activity. The most important application of RIPs is their use as immunotoxins for cancer chemotherapy[3].

2. Materials and methods

Gelonin was purified by Blue sepharose chromatography and subjected to extensive chemical modification studies[4]. Protein synthesis was assayed in a rabbit reticulocyte lysate[5]. The secondary structure of gelonin was determined by analysing the far-UV circular dichroism spectrum according to the method of Provencher and Glockner[6]. The K_a for the association of the triazine dyes with gelonin was calculated from fluorescence-quenching experiments as described by Chipman *et al*[7]. Incubation of gelonin and ribosomal RNA were carried out according to Endo *et al*[2].

3. Main results and conclusions

Gelonin was purified to homogeneity from the seeds of *Gelonium multiforum* in high yields. Analysis of the far-UV circular-dichroism spectrum of gelonin showed that the secondary structure is predominantly α-helical. Triazine dyes such as Cibacron blue F3GA and its analogue Procion blue *MX-R* coupled to sepharose have been used for a long time to purify several nucleotide-metabolising enzymes. The dyes mimic the nucleotides and hence specifically bind to the mono/polynucleotide-binding regions of several proteins[8]. The difference spectrum of Cibacron blue-F3GA with gelonin showed a typical 'electrostatic spectrum' with a maximum at 690 nm and two minima at 630 nm and 585 nm. Analysis of the quenching experiments of the intrinsic fluorescence of gelonin revealed a K_a of about $1 \times 10^6\ M^{-1}$ for all dyes tested.

Next, chemical modification studies on gelonin revealed that lysine, histidine, tyrosine, tryptophan and carboxyl groups are not required for the biological activity of gelonin. Only modification of arginine residues caused a nearly 90% loss in activity without any change in the secondary structure of the protein[4]. A time course of the reaction of gelonin with cyclohexanedione showed that the arginine residues could be classified into three groups. Modification of the first set of two residues led to little loss in activity but modifying the next set of two brought about a drastic loss in activity, with no further change on modifying the remaining six residues. Interestingly, the arginine-modified gelonin failed to bind to Cibacron blue F3GA which indicated that some of these residues may be directly binding to the negatively charged sulfonate groups of the dye. To verify this we affinity labelled gelonin with Procion blue *MX-R* and also tested its effect on polyribonucleotides and naked rRNA. The rate of inactivation of gelonin by the dye was concentration dependent and showed pseudo-first-order kinetics. A plot of the log [apparent rate constant] *vs* log [dye] has a slope of 1.05 indicating a 1:1 dye-active site complex. To establish the covalent nature of binding of the dye to protein, we synthesized a nitrene photoaffinity label by replacing one of the reactive Cl atoms in Procion blue *MX-R* with an azide group and the other with ^{125}I. Photoaffinity labelling caused an 85% loss in the protein-synthesis inhibitory activity. Taken together with the chemical modification studies it appears as though the affinity label directly modifies the essential arginine residues.

The above-mentioned studies led to the studies on the establishment of the substrate for gelonin. Gelonin appears to hydrolyse, specifically, only purine-containing homopolynucleotides such as poly(*A*) and poly(*I*) in a dose-dependent manner. Cibacron blue F3GA inhibits this activity also in a dose-dependent manner. Unlike α-sarcin which causes an extensive cleavage of 28S rRNA, both gelonin and ricin did not hydrolyse either naked 28S rRNA or 18S rRNA from monkey kidney cells. We have not been able to demonstrate an N-glycosidase activity of gelonin to show its similarity to the action of ricin *A* chain.

References

1. Barbieri, L. and Stripe, F. *Cancer Surv.*, 1982, **1**, 489–520.
2. Endo, Y., Mitsui, K., Motizuki, M. and Tsurugi, K. *J. Biol. Chem.*, 1987, **262**, 5908–5912.
3. Thorpe, P. E. and Ross, W. C. J. *Immunol. Rev.*, 1982, **62**, 119.
4. Srinivasan, Y., Ramprasad, M. P. and Surolia, A. *FEBS Lett.*, 1985, **192**, 113–118.
5. Pelham, H. R. B. and Jackson, R. J. *Eur. J. Biochem.*, 1976, **67**, 247–256.

6. PROVENCHER, S. W. AND GLOCKNER, J. *Biochemistry*, 1981, **20**, 33–37

7. CHIPMAN, D. M., GRISARO, V. AND SHARON, N. *J. Biol. Chem.*, 1967, **242**, 4388–4394

8. STELLWAGEN, E. *Acc. Chem. Res.*, 1977, **10**, 92.

Thesis Abstract (Ph.D.)

Protein – DNA interactions: A computer modelling study by B. Gopalakrishnan.
Research supervisor: Manju Bansal.
Department: Molecular Biophysics Unit.

1. Introduction

α-Helices found in the DNA-binding domains of regulatory proteins have been suggested to bind in the major groove of operator DNA and effect specific recognition[1,2]. The present study is aimed at understanding the nature and specificity of protein-DNA interactions, with particular reference to the α3 helix of λ-cro-repressor protein and its interactions with both operator and non-operator DNA sequences.

2. Method

Molecular modelling is an important tool used by the theoretical chemist to understand the structure, conformation and interaction of various molecules, small and big. With the availability of large and fast computers, molecular modelling has become synonymous with computer modelling, and it is possible to study the structure and interaction of large and complex molecular systems. Computer modelling methods have been used to study the interactions of α-helical peptides with double-helical DNA. The effect of different dielectric constants in the calculation of the electrostatic energy of biomolecules is also discussed.

3. Results

3.1 *α-Helix–DNA interactions*

The interaction of α-helical oligopeptides of various complexities, in terms of the size and charge of the side chains, *viz.*, alanine, valine and serine with DNA in the major groove are described. In the first part, results of an $(Ala)_{10}$ α-helix interaction with different base sequences in right- and left-handed *B*-DNA have been presented. The effect of allowing local structural variations on such interactions has also been studied by the molecular mechanics program AMBER for representative $(Ala)_{10}$ – DNA complexes[3]. The results of Ala-Val and $(Ser)_{10}$ α-helices interacting with right-handed *B*-DNA indicate that (1) the importance of non-specific interactions in protein α-helix – DNA interactions, (ii) a model α-helical polypeptide like $(Ala)_{10}$ can fit in the major groove of left-handed *B*-DNA also, and (iii) the α-helix taken in two orientations, NC and CN, interacts equally well in the major grooves of different DNA sequences.

3.2 Interaction of model hexapeptides with DNA

Hydrogen bonding between amino-acid side chains and DNA bases is one of the ways by which proteins can recognise specific base sequences[4]. A comprehensive analysis of the hydrogen-bonding interactions of two dipeptides containing polar residues, Asn[5] and Lys complexed with different DNA sequences in the major groove, has been carried out. Next, as a systematic build up to the λ-cro repressor $\alpha 3$ helix from a hexa-alanine α-helix, the interactions of five hexapeptides with different operators and non-operator DNA sequences have been studied. Polar amino-acid residues (Gln, Asn, Ser & Lys) are seen to form an enormous variety of hydrogen bonds with DNA bases and backbone. Substitution of these residues in the interacting α-helix leads to less stable complexes, while a change in the base sequence was not seen to affect the interaction substantially[6].

3.3 Molecular mechanics studies on λ-cro $\alpha 3$ helix–DNA interactions

To examine whether similar interaction energies in the operator and non-operator DNA complexes of λ-cro α-helix could be due to the rigid nature of the DNA and α-helix backbones, representative complexes were subjected to detailed molecular mechanics calculations using AMBER. The effect of local structural variations on the interaction of the cro-$\alpha 3$ helix with operator and non-operator DNA and a possible model for the λ-cro $\alpha 3$ helix-OR3 DNA interactions have been discussed. The results imply that the primary role of the α-helix in λ-cro repressor may be to form a stable complex with the DNA and properly orient the rest of the protein so that some other residues may effect specific recognition[6]. Calculated interproton distances in different DNA models have been compared with ^{1}H NMR nOe data from various DNA oligomers[7].

References

1. PABO, C. O. AND SAUER, R. T. — Protein-DNA recognition, *A. Rev. Biochem.*, 1984, **53**, 293–321.
2. SCHLEIF, R. — DNA-binding by proteins, *Science*, 1988, **241**, 1182–1187.
3. GOPALAKRISHNAN, B. AND BANSAL, M. — Theoretical studies on alpha helix–DNA interactions, *J. Biomol. Struct. Dynam.*, 1988, **5**, 859–871.
4. HELENE, C. AND LANCELOT, G. — Interactions between functional groups in protein-nucleic acid associations, *Prog. Biophys. Molec. Biol.* 1982, **39**, 1–68.
5. GOPALAKRISHNAN, B. AND BANSAL, M. — Modelling DNA recognition by proteins: Interaction of an Asn dipeptide with DNA, *Indian J. Biochem. Biophys.*, 1988, **25**, 495–503.
6. MANJU BANSAL AND GOPALAKRISHNAN, B. — λ-cro Repressor α_3 helix–DNA interactions – A computer modelling study. Book of Abstracts, *Sixth Conversations in Biomolecular Stereodynamics*, SUNY, Albany, NY, 1989, p 13.
7. GOPALAKRISHNAN, B. AND BANSAL, M. — Comparison of interproton distances in DNA models with nuclear Overhauser enhancement data, *J. Biosci.*, 1985, **8**, 603–614.